CONFOUNDING CONSTITUENTS

IN REMOTE SENSING OF PHYCOCYANIN

Lara Anne Vallely

Submitted to the faculty of the University Graduate School
in partial fulfillment of the requirements
for the degree
Master of Science
in the Department of Geography,
Indiana University

July 2008

Accepted by the faculty of Indiana University, in partial
fulfillment of the requirements for the degree of Master of Science.

_____

Jeffery S. Wilson, Ph.D.

Master's Thesis
Committee

_____

Lenore P. Tedesco, Ph.D.

_____

Lin Li, Ph.D.

ACKNOWLEDGEMENTS

ABSTRACT

Lara Anne Vallely

CONFOUNDING CONSTITUENTS
IN REMOTE SENSING OF PHYCOCYANIN

This project examines the impact of confounding variables that have limited the accuracy of remotely predicting phycocyanin in three Indiana drinking and recreational water reservoirs. In-situ field reflectance spectra were collected from June to November 2006 over a wide range of algal bloom conditions using an ASD Fieldspec (UV/VNIR) spectroradiometer. Groundtruth samples were analyzed for chlorophyll *a*, phycocyanin, total suspended matter, and other water quality constituents. Previously published spectral algorithms for the detection of phycocyanin were evaluated against lab measured pigment concentrations using linear least squares regression. Algorithm performance varied across study sites (best performing models by reservoir resulted in r^2 values of 0.32 to 0.84). Residuals of predicted versus measured pigment concentrations were analyzed against concentration of potential confounding water constituents. Residual analysis revealed optically active constituents contributed between 25% and 95% of original phycocyanin model errors. Inclusion of spectral variables into models to account for significant confounders resulted in improved spectral estimates of phycocyanin ($r^2 =$ 0.56 to 0.93).

Jeffrey S. Wilson, Ph.D.

TABLE OF CONTENTS

LIST OF TABLES

LIST OF FIGURES

LIST OF ABBREVIATIONS

OAC   Optically active constituent

PC   Phycocyanin

Chl *a*   Chlorophyll *a*

TSM   Total suspended matter

ISM   Inorganic suspended matter

LOI   Loss on ignition

CDOM   Colored dissolved organic matter

DOC   Dissolved organic carbon

I. INTRODUCTION

Algal blooms can cause aesthetic and ecological degradation to water reservoirs. Aesthetic problems include surface scum and algal production of taste and odor causing compounds (Chorus and Bartram, 1999). Of specific concern are blue-green (cyanobacteria) algal blooms which can threaten animal and human health (Pitois et al., 2000; Chorus and Bartram, 1999). Fish kills can result from anoxia: as algal blooms die off, cell decay leads to oxygen depletion. Human health concerns stem from potential for toxin production by some blue-green algal species. Animal deaths from toxin intake have been reported in New Zealand (Hamill, 2001) and in North and South America, Europe and Africa (Chorus and Bartram, 1999).

Cyanobacteria growth is dependent on temperature, light, and nutrient concentrations and is often associated with eutrophication (Pitois et al., 2000). Eutrophication is the process of nutrient enrichment in water bodies, particularly from phosphorous and nitrogen (Horn and Goldman, 1994). Eutrophication is a natural process, though anthropogenic activity has hastened nutrient enrichment. As nitrogen and phosphorous levels rise in water bodies, conditions become more conducive for blue-green algal blooms (Pitois et al., 2000). As such, cultural eutrophication is understood to spur the frequency of blue-green algal blooms (Chorus and Bartram, 1999; Dekker, 1993).

Because blue-green algal blooms degrade water quality, controlling their occurrence is a priority for water managers. Current monitoring practices often involve widely dispersed station sampling and lab analysis. The ephemeral nature of algal blooms makes effective monitoring in this manner difficult. Remote sensing offers an alternative to minimal station monitoring by providing a synoptic view of a feature of interest (Simis et al., 2005; Gitelson et al., 2000; Schalles and Yacobi, 2000; Gitelson et al., 1993). Phycocyanin, a pigment unique to blue-green algae and demonstrating a diagnostic spectral absorption in freshwater systems, makes the remote detection of blue-green algae possible (Simis et al., 2005; Schalles and Yacobi, 2000).

Multiple algorithms have been developed to estimate phycocyanin concentration from remote sensing data. These include models created by Simis et al. (2005), Schalles and Yacobi (2000), Dekker (1993), and Millie et al. (1992). The performance of these algorithms has only been tested on a few inland water systems with varying success. Applications to Indiana drinking water reservoirs showed model performance varied by reservoir (r^2 values ranged from 0.32 to 0.91) (Randolph, 2007; Sengpiel, 2007). A better understanding of water quality constituents that impact phycocyanin concentration estimates derived from these algorithms may be used to improve their predicative capabilities and utility to water resource managers.

This project examines the impact of confounding variables that have limited the accuracy of remotely predicting phycocyanin in three Indiana drinking and recreational water reservoirs. Previously published spectral algorithms for the detection of phycocyanin are evaluated against lab measured pigment concentrations using linear least squares regression. Residuals of predicted versus measured pigment concentrations are analyzed against concentration of potential confounding water constituents. The purpose of this analysis is twofold: to determine the extent to which other water constituents interfere with model predictions and introduce error in phycocyanin concentration estimates, and to account for confounding water constituents to improve remote sensing of phycocyanin concentration.

II. BACKGROUND

Case I verse Case II Waters

In 1977 Morel and Prieur introduced a classification of water bodies in remote sensing work based on their optical composition and complexity. Case I waters are understood to be optically simple and generally refer to open ocean waters. Phytoplankton and its byproducts dominate their spectral properties (Schalles, 2006; Morel, 2001; Bukata et al., 1995). Reflectance is understood to be a function of living algal cells, organic tripton from the death and decay of algae, and dissolved organic matter from phytoplankton metabolism and decay of organic tripton (Schalles, 2006). Case I waters are characterized by high photic depths (the depth at which irradiance is 1% of the value at the water surface) and higher concentration of algal pigments compared to other optically active constituents (Bukata et al., 1995; Morel and Prieur, 1977).

Case II waters are understood to be optically complex bodies where phytoplankton, inorganic and organic particulate matter, and dissolved organic matter all significantly impact the water's spectral signature (Morel and Prieur, 1977). Varying concentration of these optically active constituents present challenges to remote sensing of cyanobacteria (Vertucci and Likens, 1989). Unlike Case I waters, suspended matter and dissolved organic matter present in the water column are not only the product of phytoplankton but can have terrigeneous sources and be spatially heterogeneous (Schalles, 2006; Morel, 2001; Bukata, 1995; Gitelson et al., 1993). Resuspension of bottom particles, terrigenous colored dissolved organic matter, and anthropogenic particulate and dissolved substances can all impact radiance leaving a Case II water body (Schalles, 2006).

Despite challenges, remote sensing of Case II waters has become increasingly prevalent (Schalles, 2006). Most inland water systems, including those examined in the current research, are categorized as Case II. Their importance to human interests (e.g., drinking water sources, fisheries, recreational use) and their vulnerability to anthropogenic eutrophication underscore the need to monitor these water bodies timely and accurately (Yacobi, 2006; Liu et al., 2003; Dekker, 1993).

Field Water Spectra

Water constituents have spectral absorption properties that make their remote detection through spectroscopy possible. Radiance leaving a water body is a function of reflection, absorption, and transmission of the optically active constituents in a water body. Spectral properties typical of Case II waters are illustrated in Figure 1. Spectra from two study sampling points with varying concentrations of water constituents are shown.
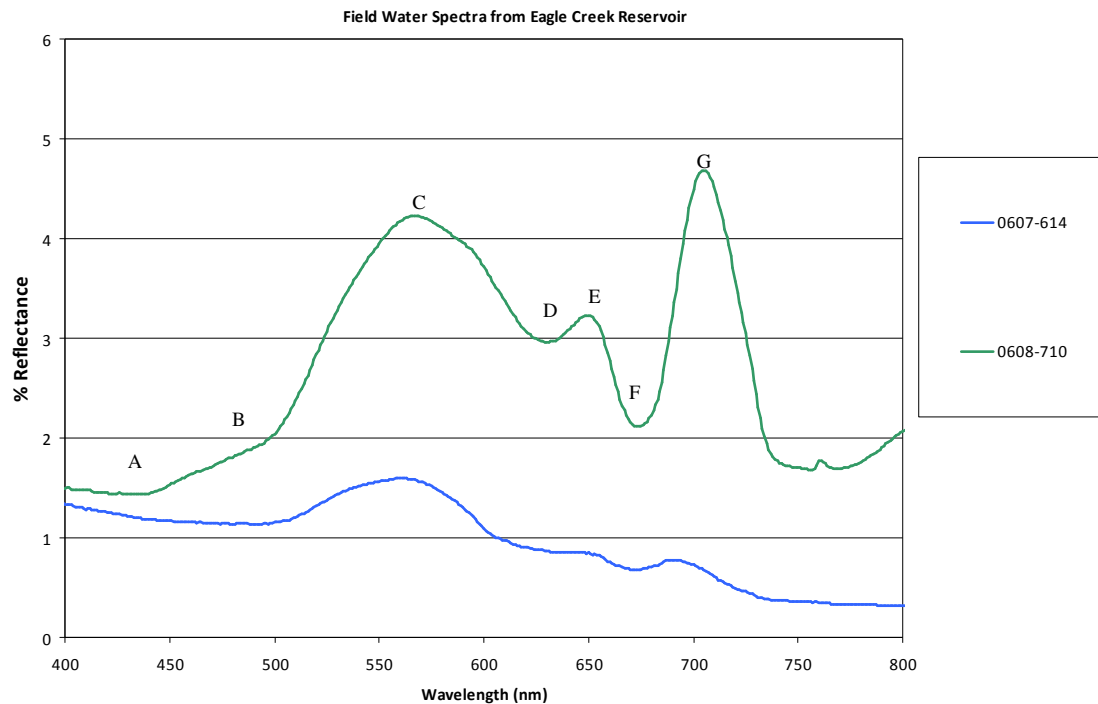
Figure 1. Field spectra of two water samples collected at Eagle Creek Reservoir in July and August 2006.

The samples have distinct spectral curves. Sample 0608-710 had lab measured phycocyanin and chlorophyll *a* pigment concentrations of 188 and 91 ppb, respectively. Sample 0607-614 had lab measured phycocyanin and chlorophyll *a* pigment concentration of 18 ppb and 15 ppb, respectively. The spectral signature from sample 0608-710 is typical of in-bloom Case II water.

Chlorophyll *a* has an absorption maximum at 440 nm, causing a characteristic reflectance dip at this value with increasing pigment concentration (A). This spectral characteristic is

4

used in the remote detection and mapping of chlorophyll *a* in Case I waters, but not in Case II waters as other water constituents (e.g., suspended sediment and colored dissolved organic matter) impact reflectance in this portion of the spectrum (400 to 500 nm) (Gitelson et al., 2000; Gitelson et al., 1993; Gitelson, 1992; Dekker et al., 1991). Carotenoid absorption results in the low reflectance values in these shorter wavelengths as well (B). The visible green peak at 550 to 570 nm (C) is a function of minimal absorption of all algal pigments. It is also impacted by scattering from algal cells and suspended sediment (Gitelson et al., 2000; Schalles and Yacobi, 2000). Peak wavelength position in this spectral region is influenced by phycocyanin concentration: higher pigment concentrations push the green peak towards lower wavelengths (Gitelson et al., 2000; Schalles and Yacobi, 2000). The trough at approximately 620 to 630 nm (D) results from the absorption maximum of phycocyanin (Simis et al., 2005; Gitelson et al., 2000; Schalles and Yacobi, 2000; Gitelson et al., 1995). This unique spectral absorption is exploited in remote sensing models to estimate phycocyanin concentration: the depth of this trough has been found to vary with blue-green algae abundance – increasing trough depth is synonymous with higher pigment concentration (Gitelson et al., 2000; Schalles and Yacobi, 2000). The reflectance peak at approximately 650 nm (E) represents phycocyanin fluorescence maximum (Rowan, 1989). The reflectance trough at approximately 670 nm (F) is the chlorophyll *a* absorption maximum; it is predominantly used in remote sensing estimations of chlorophyll *a* concentration for case II waters (Dekker, 1993; Gitelson et al., 1993; Gitelson, 1992). The distinctive reflectance peak at approximately 700 nm is a function of scattering by algal cells and particulate matter (Gitelson et al., 2000; Gitelson, 1992).

Optically Active Constituents

Optically active constituents (OACs) refer to all constituents that impact radiance leaving the water column. In addition to algal pigments (e.g., chlorophyll *a*, phycocyanin) OACs include colored dissolved organic matter and suspended matter.

Colored Dissolved Organic Matter

Colored dissolved organic material (CDOM) is decaying or decayed carbon-based material. It has been referred to in remote sensing literature as aquatic humus, gilvin, yellow substances, humic substances, and gelbstoff (Bukata et al., 1995; Dekker, 1993). CDOM originates from decomposing phytoplankton or plant material. It primarily consists of dissolved organic carbon in the form of fulvic or humic acids (Dekker, 1993). CDOM absorbs shorter wavelength light and leaves water with a yellow or tea-stained color. It is defined optically in absorption units of sample filtrate (Schalles, 2006; Dekker, 1993; Gitelson et al., 1993) though it is also reported as dissolved organic carbon (mg/L) (Schalles, 2006; Bukata et al., 1995). CDOM most strongly absorbs in shorter wavelengths; it is primarily measured in absorption units at a wavelength below 500 nm (e.g., Dekker 1993; Gitelson et al., 1993). Dekker (1993) and Vodacek et al. (1997) found significant correlation between optically measured CDOM and measures of dissolved organic carbon ($r^2 = 0.96$ and $r^2 = 0.86$, respectively).

Absorption of light by CDOM can significantly impact radiance leaving the water's surface. Absorption by CDOM is inversely related to wavelength and is described by an exponential decay curve (Schalles, 2006; Kutser et al., 2005; Dekker, 1993; Ferrari and Tassan, 1992). Despite most strongly absorbing in lower wavelengths, CDOM can reduce reflectance at all visible wavelengths and even into the lower NIR (Schalles, 2006; Fuli et al., 2004; Dekker, 1993; Ferrari and Tassan, 1992). Schalles (2006) showed that CDOM absorption had a stronger effect on the green and NIR reflectance peaks on algae laden water than the red absorption peaks in a controlled experiment. Additionally, absorption by CDOM has been shown to induce error in remotely sensed estimates of chlorophyll and suspended sediment in waters where CDOM is spatially heterogeneous (Ferrari and Tassan, 1992).

Total Suspended Matter

Total suspended matter (TSM) refers to inorganic and organic material suspended in the water column. Also referred to as seston, TSM constitutes all particulate matter suspended in the water column that does not pass through a 0.45 μm filter (Dekker,

1993). The inorganic and dead organic component of seston is referred to as tripton (Dekker, 1993). Suspended matter can include mineral particles of terrigenous origin, plankton, detritus (primarily from the decomposition of phytoplankton and zooplankton cells, but plant debris also), and particles of anthropogenic origin (Schalles, 2006; Bukata et al., 1995).

TSM can be optically diverse and may cause strong backscattering of incident radiation (Liu et al., 2003). When broken into its organic and inorganic components, the spectral characteristics of TSM are varied. Dekker (1993) reports organic tripton has absorption properties similar to CDOM. Conversely, inorganic tripton is understood to cause strong scattering and low absorption in the water column (Schalles, 2006). TSM is positively associated with turbidity and negatively associated with water clarity.

Several studies have examined the impact of varying levels of inorganic suspended matter and radiance leaving the water column. Schalles et al. (1997) conducted a controlled experiment where reflectance spectra were taken with stepwise additions of white clay to a water tank. Overall reflectance increased with each addition, though increases were nonlinear. The peak reflectance shifted from 455 nm (with no clay) to 540 nm (with 39 mg/L of clay added). Han and Rundquist (1996) compared reflectance measurements taken with stepwise additions of two different types of clay loam soil to water tanks. They found increased reflectance with increasing sediment concentration also, though reflectance increased more with additions of finer grained soil than coarser grained soil. They reported this agreed with other controlled experiments that found increased reflectance with decreased particle size (Novo et al., 1989). In addition to increases in overall reflectance, peak reflectance shifted to longer wavelengths as soil concentration increased for both textures.

Work has also been done which measures the impact of varying levels of suspended matter on the estimation of chlorophyll *a*. Han et al. (1994) conducted a controlled experiment where suspended sediment was incrementally added to algal chlorophyll and water. Their results indicated an increase in overall reflectance values with increasing

levels of suspended sediment, though the unique spectral characteristics of chlorophyll *a* remained intact despite changing sediment concentrations. Both the chlorophyll *a* red absorption maximum (approximately 670 nm) and the NIR reflection maximum (approximately 700 nm) were minimally affected by changing levels of sediment, and the use of the commonly used NIR/red ratio to estimate chlorophyll remained robust. Schalles et al. (1997) conducted a similar experiment where suspended sediments were incrementally added to a tank with a controlled level of chlorophyll *a*. They found increasing levels of suspended sediments influenced the wavelength position of reflectance peaks. Their work confirmed the need to use hyperspectral sensor to accurately remotely sense pigment concentrations in waters with varying levels of suspended sediments. Work measuring the impact of varying levels of suspended sediment on the remote estimation of phycocyanin has not been documented.

Model Types

Water quality remote sensing models use reflectance values (R) at specific wavelengths (λ) following:

$$R = [L_u(\lambda)] * [E_d(\lambda)]^{-1} \qquad\qquad \text{Equation 1}$$

where,
L_u = upwelling radiance measured above or below the water surface
E_d = downwelling irradiance

Reflectance values at wavelengths sensitive to changes in concentration of the OAC of interest are utilized. Morel and Gordon (1980) classified water quality remote sensing models into three different types: empirical, semi-empirical, and bio-optical.

Empirical methods derive relationships between spectra and measured water quality concentrations through statistical analysis. Development of these algorithms requires simultaneous collection of spectral and water quality data. Empirical models are often straightforward, though they lack transferability (Strombeck, 2001). Empirical relationships are site-specific and models have less predictive power when used for other water bodies (Dekker, 1993). Empirical models for the detection of pigments typically

incorporate reflectance at multiple wavelengths as independent variables in regressions to estimate pigment concentration. Models are typically in the form of:

$$y = ax + b \qquad \text{Equation 2}$$

where,
y = pigment concentration
x = wavelength or wavelength ratio
a and b = model coefficients

Bio-optical models utilize inherent and apparent optical properties (IOPs and AOPs) of a water body. Inherent optical properties refer to properties that do not change with respect to changes in irradiance (Gordon et al., 1975). In optical models, reflectance under the water surface ($R(0-)$) is understood to be a function of the backscattering (b_b) and absorption coefficients (a) of the water body and its constituents, and of the light field (f) (Gons, 1999; Morel and Gordon, 1980; Gordon et al., 1975).

$$R\,(0\text{-}) = f * b_b / (a + b_b) \qquad \text{Equation 3}$$

The concentration of the constituent of interest is derived through the inverse modeling of the absorption and backscattering coefficients of the water and its constituents. The absorption coefficient of the constituent of interest is divided by its specific absorption coefficient ($a*$), absorption per unit path length and mass concentration, yielding concentration (Simis et al., 2005).

$$a / a* = \text{constituent concentration} \qquad \text{Equation 4}$$

In bio-optical models for Case II waters, total absorption (a) is understood to be a function of absorption from all the optically active constituents in the water column: phytoplankton (a_{ph}), water (a_w), CDOM (a_{CDOM}), and suspended sediment (a_{ss}) (Gons, 1999):

$$a_{total} = a_{ph} + a_w + a_{CDOM} + a_{ss} \qquad \text{Equation 5}$$

Thus to utilize bio-optical models in these systems, IOPs and AOPs are needed for all optically active water constituents.

Semi-empirical models incorporate components of both bio-optical and empirical models. IOPs and AOPs are used in addition to statistical relationships between estimated and *in-situ* water quality data. An example of this method is given by Simis et al. (2005). Their semi-empirical model, developed to predict phycocyanin, utilized absorption properties of phycocyanin in addition to linear least square optimization coefficients.

Phycocyanin Algorithms

This study examines previously published empirical algorithms developed for the detection of phycocyanin concentration in inland water. Modifications of four models are utilized (Simis et al., 2005; Schalles and Yacobi, 2000; Gitelson et al., 1995; Dekker, 1993).

Table 1. Empirical algorithms used in analysis.

Empirical Algorithms	Source
R_{709} / R_{620}	Modified from Simis et al., 2005
R_{650} / R_{625}	Schalles and Yacobi, 2000
R_{624}	Gitelson et al., 1995
$0.5(R_{600} + R_{648}) - R_{624}$	Dekker, 1993

In addition to these empirical algorithms, a semi-empirical model proposed by Simis et al. (2005) is assessed. This algorithm incorporates inherent optical properties of the water column into its phycocyanin predictions as:

$$a_{pc(620)} = ((\{[R_{709} / R_{620}] * [aw_{709} + b_b]\} - b_b - aw_{620}) / \delta) - [\varepsilon * a\text{chl}_{665}] \qquad \text{Equation 6}$$

where,
$a_{pc(620)}$ = absorption of phycocyanin at 620 nm

$$a\text{chl}_{665} = (\{[R_{709} / R_{665}] * [aw_{709} + b_b]\} - b_b - aw_{665}) / \gamma \qquad \text{Equation 7}$$

$a\text{chl}_{665}$ = absorption of chlorophyll *a* at 665 nm

R_λ = reflectance value at a specified wavelength

aw_λ = pure water absorption coefficients at a specified wavelength
aw_{709} = 0.70 m^{-1} (Buitevled et al., 1994)
aw_{665} = 0.40 m^{-1} (Pope and Fry, 1997)
aw_{620} = 0.30 m^{-1} (Buitevled et al., 1994)

δ = an optimization constant derived from a linear least-squares regression of measured to estimated phycocyanin absorption, 0.84 (Simis et al., 2005)
γ = an optimization constant derived from a linear least-squares regression of measured to estimated chlorophyll *a* absorption, 0.68 (Simis et al., 2005)
ε = a conversion factor to account for chlorophyll absorption at 620nm relative to 665, 0.24 (Simis et al., 2005)

b_b = backscattering coefficient obtained from method proposed by Astoreca (2006)
b_b = (aw $_{778}$ α R_{778}) / (γ' - α R_{778})
$aw778$ = 2.69 m^{-1} (Buiteveld et al., 1994)
γ' = an empirical constant, 0.082
α = a factor relating to refraction and reflection at the water surface, 0.60.

Pigment concentration is obtained by dividing the measured absorption at the specified

wavelength to the appropriate specific absorption coefficient:

$a$pc$_{620}$ / a^*_{620} = phycocyanin concentration in mg / m^3 Equation 8
$a$chla $_{665}$ / a^*_{665} = chlorophyll *a* concentration mg / m^3 Equation 9

where,
a^*_{620} = 0.0095 m^2 / mg (Simis et al., 2005)
a^*_{665} = 0.0153 m^2 (Simis et al., 2005)

III. MATERIALS AND METHODS

General Study Design

A field campaign was carried out during the summer and fall of 2006 on three central Indiana reservoirs. Ground truth water samples were collected simultaneously with field spectral measurements within a range of algal bloom conditions. Water samples were analyzed for a variety of water quality parameters. The study was designed to confirm relationships established between field spectra and algal pigment concentration (Randolph, 2007; Sengpiel, 2007) while also assessing the influence of additional water quality parameters on the robustness of these relationships.

Study Sites

Eagle Creek, Geist, and Morse Reservoirs are the focus of this study. These reservoirs are part of a drinking and recreational water system for the city of Indianapolis, Indiana, USA and the surrounding communities. Water managers have reported algal blooms in all three reservoirs (Li et al., 2006; Tedesco et al., 2003). A summary of reservoir characteristics is given in Table 2.

Table 2. Reservoir characteristics (Li et al., 2006).

Reservoir	Eagle Creek	Geist	Morse	Units
Original Purpose	Flood Control	Water Supply	Water Supply	
Date of Service	1968	1943	1956	
Surface Area	1.9	2.9	2.3	mi^2
Reservoir Volume	5,500	6,300	7,400	million gallons
Maximum Depth	54	48	42	ft
Mean Depth	13' 9"	10' 6"	15' 5"	ft in
Residence Time	56	55	70	days
Watershed Area above Dam	162	215	227	mi^2
Trophic Status	Mesotrophic-Eutrophic	Mesotrophic	Eutrophic	
% Agriculture in Watershed	60.1%	58.3%	76.9%	

Eagle Creek Reservoir

Eagle Creek Reservoir was constructed by the city of Indianapolis by 1967 to control flooding along Eagle Creek. It is fed by a 162 square mile watershed. Land use in the watershed is predominantly agricultural (60.1%) with some sub-watersheds transitioning to suburban development (Li et al., 2006; Tedesco et al., 2003). The reservoir is used for recreational purposes (e.g. swimming, boating, fishing) and is bordered by Eagle Creek Park. In 1976 a direct intake was established in the reservoir which serves the T.W. Moses water treatment facility. It is the only reservoir in the study to serve a direct intake to a water treatment facility. The direct intake has been problematic, as taste and odor compounds caused by algal blooms in the reservoir are not mitigated before treatment (Tedesco et al., 2003).

Morse Reservoir

Morse Reservoir was constructed between 1953 and 1956 by the Indianapolis Water Company. Its original purpose was to provide consistent water supply to the water company's White River water treatment facility. Morse Reservoir is fed by the Cicero Creek watershed, a 214 square mile watershed where 76.9% of the land use is agricultural (Li et al., 2006; Tedesco et al., 2003). Land use immediately surrounding Morse Reservoir is predominantly residential. It is used recreationally by the community for swimming, boating, and fishing. Due to its eutrophic nature, Morse Reservoir has experienced degrading algal blooms that produce problematic taste and odor compounds (Tedesco et al., 2003).

Geist Reservoir

Geist Reservoir was also constructed by the Indianapolis Water Company to provide a consistent water supply to one of the company's water treatment facilities. Construction of the reservoir was completed in 1944. Geist Reservoir is fed by the 219 square mile Fall Creek watershed (Tedesco et al., 2003). Nearly 60% of land use in the watershed is agricultural (Li et al., 2006). Real estate development began around the reservoir in the early 1980s, and today nearly all of its shoreline is composed of residential land use. Geist Reservoir is used recreationally for swimming, boating, and fishing. Like Eagle

Creek and Morse, Geist Reservoir has experienced degrading algal blooms due to its eutrophic nature (Tedesco et al., 2003).

Data Collection

A field campaign was carried out from June through November 2006. Samples were taken under a diverse range of algal bloom conditions (chlorophyll *a* and phycocyanin concentrations ranged from 2.69 to 182.55 and 0.73 to 370.95 ppb, respectively). A summary of samples taken is given in Table 3.

Table 3. Summary of spectra and water samples collected by reservoir with corresponding lab analysis performed.

Date	Spectra samples taken	Spectra Samples Retained	OACs measured				Samples Used in Analysis	
			PC	Chl *a*	ISM	DOC	Both PC and Spectra values (Phases 1 and 4)	All Parameters measured (Phases 2 and 3)
Eagle Creek Reservoir								
15-Jun-2006	26	19	11	12	11	11	8	8
20-Jun-2006	23	20	9	8	9	10	7	4
29-Jun-2006	11	6	10	11	8	11	5	5
6-Jul-2006	11	9	11	11	5	11	9	4
25-Jul-2006	11	11	11	9	11	11	10	9
16-Aug-2006	21	21	20	20	21	15	20	14
23-Aug-2006	18	17	18	18	16	0	17	0
2-Nov-2006	5	5	5	5	0	0	5	0
Total	*126*	*108*	*95*	*94*	*81*	*69*	*81*	*44*
Morse Reservoir								
19-Jul-2006	20	16	18	19	20	20	15	14
31-Jul-2006	19	19	17	19	19	7	17	7
22-Aug-2006	20	20	17	19	20	0	17	0
19-Sep-2006	2	2	2	2	0	0	2	0
25-Sep-2006	19	19	16	18	0	9	16	0
6-Oct-2006	21	20	20	20	0	8	19	0
Total	*101*	*96*	*90*	*97*	*59*	*44*	*86*	*21*
Geist Reservoir								
24-Jul-2006	16	0	15	15	16	16	0	0
1-Aug-2006	12	11	12	12	11	12	11	11
17-Aug-2006	15	15	15	15	15	0	15	0
24-Aug-2006	20	19	20	20	20	0	19	0
7-Sep-2006	16	15	13	16	15	10	12	7
26-Sep-2006	7	7	7	7	0	7	7	0
7-Oct-2006	20	18	18	20	0	0	16	0
Total	*106*	*85*	*100*	*105*	*77*	*45*	*80*	*18*
Abbreviations	PC = Phycocyanin, Chl *a* = Chlorophyll *a*, ISM = Inorganic Suspended Matter, DOC = Dissolved Organic Carbon							

Reflectance spectra were collected with an ASD FieldSpec ultraviolet/visible and near-infrared spectroradiometer (Analytical Spectral Devices Inc., Boulder, CO, USA) which collects a continuous range of electromagnetic spectrum from 350 to 2500 nm in 2150 bands. A fiber optic cable connected to the sensor was attached to an extendable pole pointed in a nadir viewing angle, approximately 1 meter above the water surface. Downwelling irradiance was measured at each sampling site using a Spectralon reference panel (Labsphere Inc., North Sutton, NH, USA) to calibrate upwelling radiance measured from the water surface (Equation 1). To reduce noise in the spectra, final reflectance values at each site were averaged over 10 consecutive readings.

Because field spectra were collected at nadir and close to solar noon, specular reflectance off of the water surface impacted some spectra samples. All spectra were visually assessed for quality and samples with extensive noise or overtly high reflectance values (greater than 15%) were not included in data analysis. Numbers of samples taken and retained are presented in Table 3.

In situ water measurements were collected with a YSI 600 XLM multi-parameter probe (YSI Inc., Yellow Springs, OH, USA). Measured *in situ* variables included temperature, specific conductivity, total dissolved solids, salinity, dissolved oxygen, and pH. GPS coordinates were collected at each in situ sampling location and water clarity was estimated using a Secchi disk.

Surface water grab samples were collected at each sampling location approximately 0.3 meters below the water surface. Samples collected were analyzed for phycocyanin, chlorophyll *a*, total suspended matter, and loss on ignition (LOI) at Indiana University-Purdue University Indianapolis. Replicates for phycocyanin, chlorophyll *a*, suspended matter, and LOI analysis were taken. Samples with greater than 20% error (mean / standard deviation) between replicates were excluded from further analysis. Dissolved organic carbon (DOC) and secondary chemical analysis were performed by Veolia Water laboratories (Indianapolis, IN, USA) following Environmental Protection Agency and American Public Health Association standards (Appendix A).

Analytical Methods

Pigment Analysis

Samples analyzed for pigment concentration were collected in 1 L amber HDPE bottles. At collection, samples were placed on ice and then filtered and frozen within four to eight hours. All steps of the phycocyanin and chlorophyll *a* analysis were performed in subdued lighting conditions.

Phycocyanin

Water samples were analyzed for phycocyanin following Sarada et al. (1999). 150 to 300 ml of sample was filtered through a Millipore 47 mm glass fiber filter within 8 hours of collection. Filters were transferred to 15 mL falcon tubes, stored in a dark freezer, and remained frozen until extraction. Filters were transferred to 50 mL polycarbonate centrifuge tubes and suspended in 15 mL of 50mM phosphate buffer. Filters were broken up using a stainless steel spatula and then underwent two grinding and centrifuge cycles. Centrifuging was done at 5° C, 27,000 * g for 25 minutes using a Beckman J2-21M centrifuge. Extract was analyzed for phycocyanin concentration fluoremetrically with a TD-700 Fluorometer (Turner Designs, Inc.) using a Cool White Mercury Vapor Lamp and a Phycocyanin Optical Kit (630 nm excitation and 660 nm emission filters). The fluorometer was first calibrated using C-phycocyanin from Spirulina sp. (Sigma-Aldrich P6161). Measured phycocyanin concentration using this extraction method has shown strong correlation ($r^2 = 0.946$) to blue green algal biovolume measurements (Li et al., 2006).

Chlorophyll a

150 to 200 mL of sample was filtered through 47 mm 0.45 micron pore size acetate filters. Filters were transferred to 15 mL falcon tubes, stored in a dark freezer, and remained frozen until extraction. Prior to analysis, filters were dissolved in 10 mL of 90% buffered acetone and extracted in a dark freezer for between 24 hours and 48 hours. Extract was analyzed following EPA Method 445.0 (EPA, 1997). After a 1:5 or 1:10 dilution, pheophytin corrected chlorophyll *a* was measured fluoremetrically with a TD-700 Fluorometer (Turner Designs, Inc., Sunnyvale, CA, USA) equipped with a Daylight

White Lamp and Chlorophyll Optical Kit (340 – 500 nm excitation filter and emission filter > 665nm). The fluorometer was first calibrated with chlorophyll *a* from spinach standard (Sigma-Aldrich 10865).

Total Suspended Matter (TSM)

Samples analyzed for TSM were collected in 1 L HDPE bottles. 200 – 600 mL of sample was filtered onto pre-ashed, pre-weighed 47 mm, 0.7 micron pore size glass fiber filters using a filtration manifold. Filters were dried in a 60º C oven for at least one hour before cooling in a dessicator and weighing. TSM in mg/L was calculated by subtracting the original weight of the clean filter from the post-filtered weight.

Loss on Ignition (LOI) and Inorganic Suspended Matter (ISM)

Filters used to measure TSM were weighed and then ashed for 75 minutes at 550º C in porcelain crucibles. Samples were cooled in a dessicator and weighed. Inorganic suspended matter (ISM) in mg/L was calculated by subtracting the original weight of the filter from the weight post-ashing. Loss on ignition (LOI) in mg/L was calculated by subtracting the pre-ashed weight of the filter with sample from the post-ashed weight.

Data Analysis

Four phases of analysis were completed:

1) Evaluation of previously published remote sensing algorithms developed to predict phycocyanin concentration in Case II waters. Algorithms were applied to individual reservoir data sets and evaluated through bivariate regression.

2) Identification of confounding OACs through exploratory analysis and multivariate regression of model residuals from Phase 1.

3) Inclusion of spectral estimates of significant OACs from Phase 2 into multivariate models to improve phycocyanin concentration estimates. Models developed on subsets of individual reservoir and aggregated data sets.

4) Validation of best performing models from Phase 3 on subset of individual reservoir and aggregated data sets.

The number of samples used in each stage of the analysis is given in the last columns of Table 3.

Phase 1: Evaluation of previously published algorithms

Spectra were divided by reservoir and reflectance at each model's specified wavelengths was used. Because the tested algorithms are designed to use bands of maximum reflectance and absorption that correspond to algal optical properties, wavelength band ranges were examined instead of single band values to improve algorithm performance. The maximum and minimum reflectance values of a single band were used within the specified ranges given in Table 4 for the Schalles and Yacobi and modified Simis et al. ratio algorithms and the Gitelson et al. algorithm.

Table 4. Modification of three empirical algorithms.

Published Algorithm	Modified
R_{650} / R_{625}, Schalles and Yacobi, 2000	$R_{\max \lambda (645\text{-}655)}$ / $R_{\min \lambda (620\text{-}630)}$
R_{709} / $_{620}$, Simis et al., 2005	$R_{\max \lambda (704\text{-}714)}$ / $R_{\min \lambda (615\text{-}625)}$
R_{624}, Gitelson et al., 1995	$R_{\min \lambda (619\text{-}629)}$

Algorithm values were graphed against analytically measured phycocyanin concentrations and a best fit line was developed to predict phycocyanin concentration at each sampling point. The coefficient of determination and root mean square error (RMSE) in parts per billion (ppb) were calculated for each reservoir.

Phase 2: Evaluation of Confounding Water Constituents

In order to assess the impact of confounding water quality parameters on the remote sensing algorithms, residuals (e_i) were computed for all of the models as:

$$e_i = y_i - \hat{y}_i$$ Equation 10

where ,
y_i = measured pigment concentration
$\hat{y}_i$ = estimated pigment concentration

Residuals were investigated in two ways. Residuals for each model were correlated with the measured OACs individually to investigate potential relationships. To measure the impact of each OAC while holding the effect of the other constituents constant, residuals were then analyzed through multivariate regression. Models were developed using residuals as the dependent variable and concentrations of known optically active constituents as predictor variables: phycocyanin, chlorophyll *a*, inorganic suspended matter, and dissolved organic carbon. Dissolved organic carbon (DOC) is included as a proxy for colored dissolved organic matter (CDOM). The purpose of this analysis was to determine the error introduced into model predictions from the optically active constituents in the water column. Because not all of the OACs were measured for each sample in the data set, the number of samples in this stage of the analysis dropped relative to Phase 1 (n = 44, 21, and 18 for Eagle Creek, Morse, and Geist Reservoirs, respectively).

Phases 3 and 4: Inclusion of confounding constituents into improved models to predict phycocyanin

In Phase 3, previously published remote sensing algorithms designed to estimate OACs that were found to be significant covariates of residuals in Phase 2 were included as independent variables with phycocyanin algorithms in multivariate regression models. The intent was to investigate if improved estimates of phycocyanin concentration could be derived by accounting for confounding constituents. Phase 3 uses the same samples analyzed in Phase 2 as training sets to create phycocyanin algorithms (given in Table 3; n = 44, 20, 18, and 82 for Eagle Creek, Morse, Geist Reservoirs, and an aggregated data set, respectively). The regression coefficients developed in Phase 3 are applied to a new subset of samples not incorporated in the model's development (given in Table 3). Only models that showed significant improvement when accounting for confounding OACs are validated in Phase 4. Validation is done by reservoir and on an aggregated data set. The performance on the validation data sets informs how well these new models are able to predict phycocyanin.

IV. RESULTS AND DISCUSSION

Phase 1: Evaluation of previously published algorithms

Algorithm performance, by reservoir, is given in Table 5.

Table 5. Summary of spectral model performance.

Algorithm	Source	r^2	RMSE	Equation
Eagle Creek Reservoir, n = 81				
R_{709} / R_{620}	Simis et al., 2005	0.84	27.37	233.48x - 191.44
R_{650} / R_{625}	Schalles and Yacobi, 2000	0.70	37.25	873.22x – 863.02
R_{624}	Gitelson et al., 1995	0.08	65.26	-1591.06x + 94.68
$0.5(R_{600} + R_{648}) - R_{624}$	Dekker, 1993	0.74	34.54	51211.79x – 40.56
$a_{PC}(620)/a*_{PC}(620)$	Simis et al., 2005	0.84	27.49	3.37x – 47.16
Morse Reservoir, n = 86				
R_{709} / R_{620}	Simis et al., 2005	0.71	42.90	243.856x – 205.886
R_{650} / R_{625}	Schalles and Yacobi, 2000	0.61	49.56	809.91x – 794.86
R_{624}	Gitelson et al, 1995	0.07	76.35	-1359.49x +121.07
$0.5(R_{600} + R_{648}) - R_{624}$	Dekker, 1993	0.38	62.38	74504.88x – 99.57
$a_{PC}(620)/a*_{PC}(620)$	Simis et al., 2005	0.75	39.69	2.93x – 34.95
Geist Reservoir, n = 80				
R_{709} / R_{620}	Simis et al., 2005	0.32	41.20	261.21x – 226.24
R_{650} / R_{625}	Schalles and Yacobi, 2000	0.14	46.21	824.32x – 774.28
R_{624}	Gitelson et al., 1995	0.28	42.32	-2144.38x + 147.29
$0.5(R_{600} + R_{648}) - R_{624}$	Dekker, 1993	0.26	42.99	-37963x + 186.93
$a_{PC}(620)/a*_{PC}(620)$	Simis et al., 2005	0.32	40.99	2.79x – 30.32

The two Simis et al. algorithms resulted in the highest r^2 values for all three reservoirs, but model performance varied by reservoir. Best results occurred on Eagle Creek Reservoir. Both Simis et al. equations resulted in r^2 values of 0.84. Root mean square error ranged from 27 ppb for the Simis et al. equations to over 60 ppb when using reflectance values at 624 nm. Both the Schalles and Yacobi algorithm and the Dekker algorithm performed relatively well on Eagle Creek, with r^2 values of 0.70 and 0.74 respectively.

Morse Reservoir r^2 values ranged from 0.07 to 0.75, and RMSE exceeded results observed for Eagle Creek for all of the spectral models. Highest r^2 values for Morse were obtained using the Simis et al. semi-empirical algorithm (0.75), though RMSE was 40 ppb. As with Eagle Creek, the Gitelson algorithm had the highest RMSE (76 ppb) and lowest r^2 (0.07). The spectral ratios R_{709} / R_{620} and R_{650} / R_{625} resulted in r^2 values of 0.71 and 0.61, respectively.

The models performed most poorly on Geist Reservoir. r^2 values were lower for all of the models compared to their performance on Eagle Creek and Morse. The model using reflectance values at 624 nm resulted in r^2 values of 0.28, compared to 0.08 and 0.07 on Eagle Creek and Morse, respectively. The highest r^2 values for Geist Reservoir data were obtained using both Simis et al. models (r^2 = 0.32).

Phase 2: Evaluation of Confounding Water Constituents
Exploratory Residual Analysis
Optically active water quality parameters were correlated to each other and to Phase 1 model phycocyanin residuals (Table 6).

Table 6. Correlation matrix between optically active water quality parameters and model residuals by reservoir. Relationships between OACs where r > 0.70 are bolded.

	PC (ppb)	Chl a (ppb)	TSM (mg/L)	LOI (mg/L)	ISM (mg/L)	DOC (mgC/L)	R_{709} / R_{620} PC Residual	R_{650} / R_{625} PC Residual	R_{624} PC Residual	0.5(R_{600} + R_{648}) - R_{624} PC Residual	$a_{PC}(620)$ / $a*_{PC}(620)$ PC Residual
Eagle Creek Reservoir											
PC (ppb)		**0.802**	0.681	**0.829**	0.477	-0.104	0.403	0.548	**0.960**	0.508	0.404
Chl a (ppb)	0.802		**0.724**	**0.823**	0.566	-0.084	0.206	0.533	0.739	0.229	0.276
TSM (mg/L)	0.681	0.724		**0.919**	**0.927**	-0.190	-0.061	0.392	0.690	0.123	-0.080
LOI (mg/L)	0.829	0.823	0.919		**0.704**	-0.168	0.007	0.339	0.812	0.219	0.024
ISM (mg/L)	0.477	0.566	0.927	0.704		-0.149	-0.094	0.405	0.504	-0.011	-0.133
DOC (mgC/L)	-0.104	-0.084	-0.190	-0.168	-0.149		-0.124	0.229	0.174	0.326	-0.412
Morse Reservoir											
PC (ppb)		0.593	0.352	0.578	0.414	0.227	0.542	0.626	**0.964**	0.788	0.501
Chl a (ppb)	0.593		0.645	**0.727**	0.596	0.125	-0.115	0.543	0.606	0.394	-0.095
TSM (mg/L)	0.352	0.645		**0.972**	**0.973**	-0.124	-0.238	0.639	0.420	0.153	-0.176
LOI (mg/L)	0.578	0.727	0.972		**0.891**	0.379	-0.232	0.626	0.592	0.392	-0.223
ISM (mg/L)	0.414	0.596	0.973	0.891		0.110	-0.289	0.588	0.448	0.177	-0.293
DOC (mgC/L)	0.227	0.125	-0.124	0.379	0.110		-0.019	-0.165	0.036	0.287	0.141
Geist Reservoir											
PC (ppb)		0.435	-0.233	0.383	-0.581	0.637	0.826	0.927	**0.849**	0.862	0.822
Chl a (ppb)	0.435		0.137	0.672	-0.124	0.318	0.211	0.547	0.413	0.413	0.287
TSM (mg/L)	-0.233	0.137		0.023	**0.957**	-0.410	-0.293	-0.148	0.119	0.042	-0.404
LOI (mg/L)	0.383	0.672	0.023		-0.268	0.660	0.178	0.451	0.394	0.312	0.199
ISM (mg/L)	-0.581	-0.124	0.957	-0.268		-0.683	-0.693	-0.616	-0.354	-0.309	-0.698
DOC (mgC/L)	0.637	0.318	-0.410	0.660	-0.683		0.432	0.515	0.557	0.602	0.344

Correlation between the optically active water quality parameters varied by reservoir. Optically active constituents were most highly correlated in Eagle Creek Reservoir: phycocyanin was significantly correlated ($r > 0.70$) to chlorophyll a, TSM, and LOI. This is in contrast to Morse and Geist Reservoirs. Phycocyanin did correlate to chlorophyll a and LOI greater than 0.57 for Morse Reservoir. This is not as strong as the relationships revealed in Eagle Creek, but it is a much stronger relationship than phycocyanin correlation to chlorophyll a or any form of suspended matter on Geist Reservoir.

The correlations of the OACs also revealed stark differences in the nature of suspended matter amongst the reservoirs. Total suspended matter was highly correlated to both suspended matter lost on ignition (suspended organic matter in the water column) and ISM for Eagle Creek and Morse Reservoirs. The positive nature of this strong relationship reveals that areas in these reservoirs with high LOI also have high ISM (correlation coefficient between LOI and ISM for Eagle Creek and Morse Reservoirs are 0.704 and 0.891, respectively). In contrast, TSM for Geist Reservoir is only strongly correlated to ISM ($r = 0.957$) and not LOI ($r = 0.023$), and ISM and LOI are not correlated to each other ($r = -0.268$).

Relationships between TSM and LOI for all the reservoirs are plotted in Figure 2. The strong linear relationship between TSM and LOI for Eagle Creek and Morse Reservoirs (Figure 2a and b) contrasts with the weak relationship evident in the Geist scatter plot (Figure 2c). From the Eagle Creek and Morse plots it can be deduced that suspended matter in the water column is consistently a function of the organic component. Coupled with the high correlation between LOI and pigment concentration in these reservoirs (Table 6) and the consistently better performing remote sensing models of phycocyanin, it is likely that the suspended matter in these reservoirs is consistently a function of phytoplankton. This is in contract to Geist Reservoir, where it is apparent total suspended matter is not a function of the organic component in the water column (Figure 2c, Table 6). Additionally, phycocyanin is not highly correlated to LOI for Geist

Reservoir (r = 0.383) in comparison to Eagle Creek and Morse Reservoirs (r = 0.829 and 0.578, respectively).

A - Eagle Creek Reservoir

$y = 1.74x - 2.80$

$r^2 = 0.84$

TSM (mg/L) vs LOI (mg/L)

B - Morse Reservoir

$y = 1.91x - 5.91$

$r^2 = 0.94$

TSM (mg/L) vs LOI (mg/L)
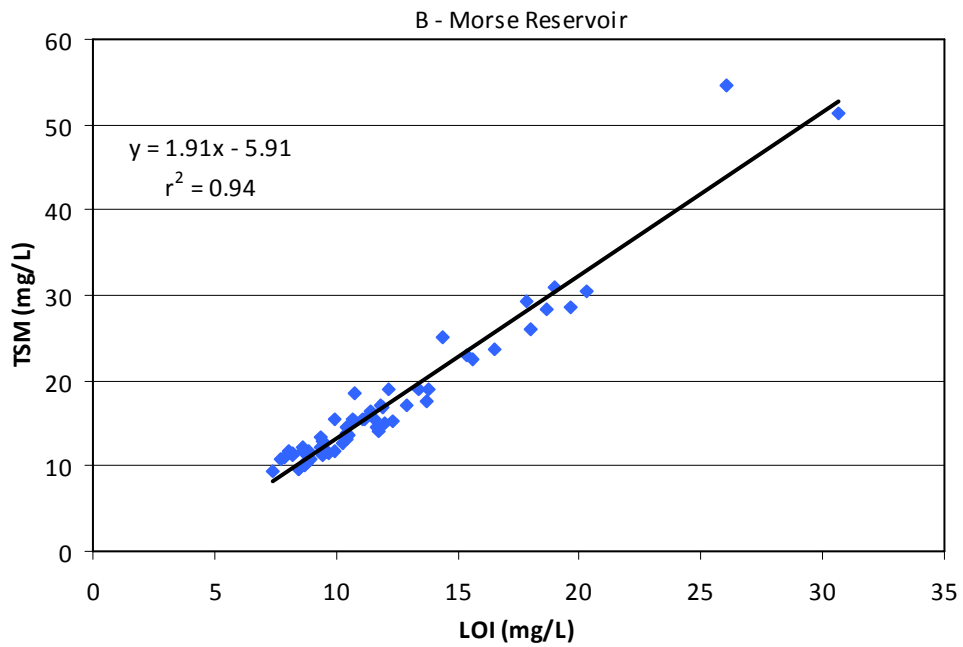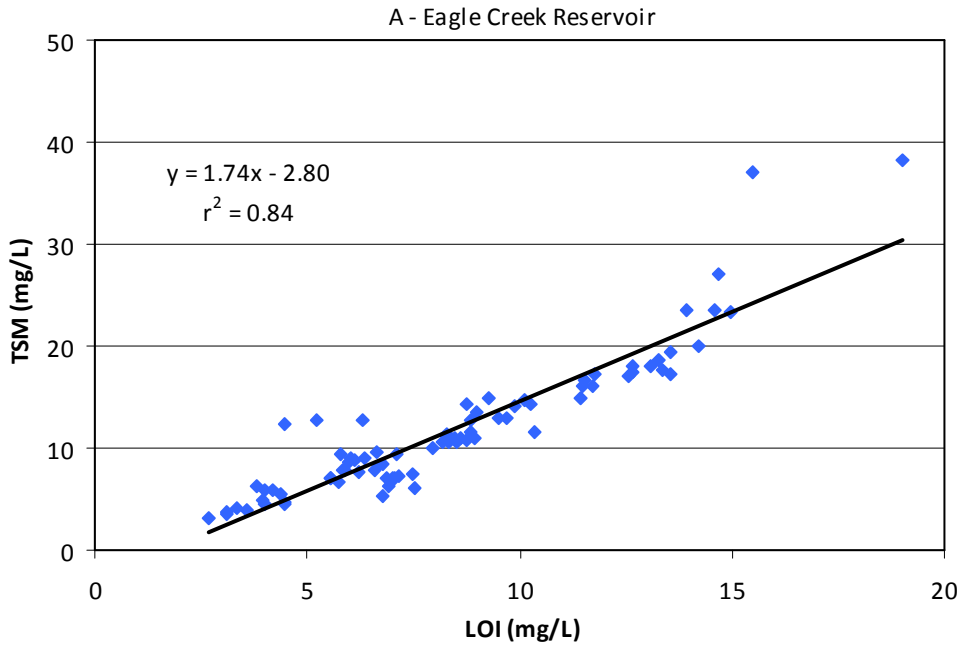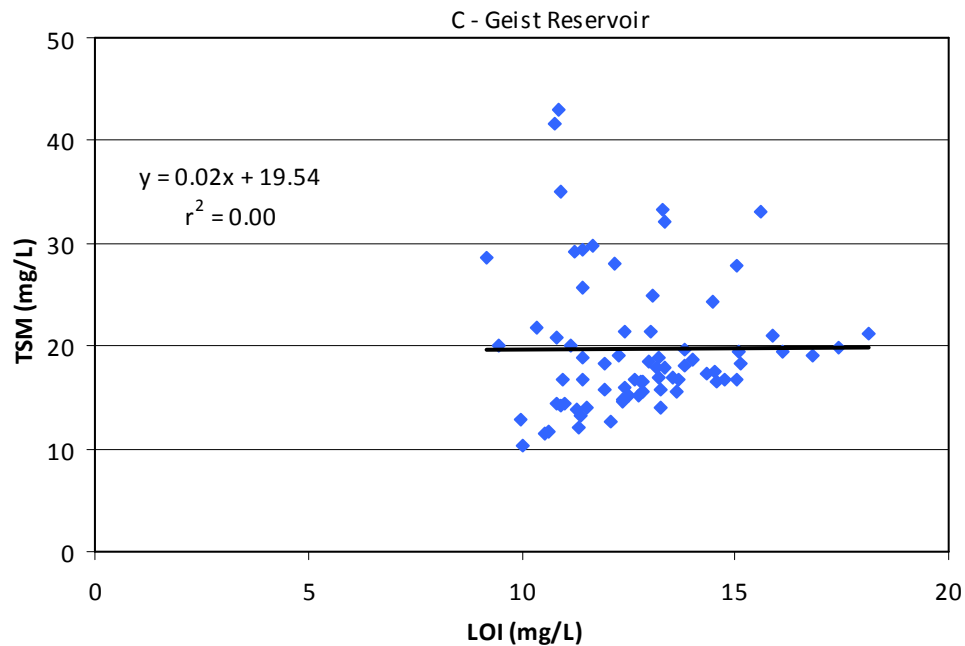
Figure 2a, b, and c. Total suspended matter verse organic suspended matter for (a) Eagle Creek, (b) Morse, and (c) Geist Reservoir.

Correlating OACs to phycocyanin spectral model residuals revealed additional relationships (Table 6). Positive correlation coefficients are associated with the underestimation of phycocyanin, and negative correlation coefficients are associated with the overestimation of phycocyanin. For the following plots of model residuals and an OAC (Figures 3, 4, 5, and 6), y-values greater than zero represent a sample where phycocyanin was underestimated, and y-values less than zero represent a sample where phycocyanin was overestimated.

Notably, phycocyanin concentration was consistently underestimated as pigment concentration increased (Table 6, e.g. Figure 3). In their work remotely sensing chlorophyll *a*, Gitelson et al. (2000) note absorption by chlorophyll *a* at 670 nm does not decrease reflectance values at 670 nm once chlorophyll *a* concentration reaches 20 mg/m^3. At this concentration, chlorophyll *a* absorption is offset by scattering from algal cells walls. Gitelson et al. (2000) state this is why the inclusion of the near infrared reflectance peak is vital in remotely sensing chlorophyll *a* in Case II water bodies at high

concentrations. The magnitude of the near infrared peak is influenced by scattering from all suspended matter, including phytoplankton biomass. Gitelson et al. note the near infrared peak is related to chlorophyll *a* concentration because of the link between pigment concentration and algal biomass.

Phycocyanin has only 20% of the absorption per unit of pigment when compared to chlorophyll *a* (Rowan, 1989). Considering phycocyanin absorbs light less effectively than chlorophyll *a*, it is possible the same dynamic Gitelson et al. (2000) describe for chlorophyll *a* occurs with phycocyanin, perhaps to an even greater extent. The phycocyanin reflectance trough (approximately 620 nm) may not deepen after a phycocyanin concentration of a certain threshold because it is also offset from scattering by algal cells.

This is related to what is known as the "package effect." Because pigments are contained in discrete packages their light harvesting efficiency is lower than if uniformly distributed within a solution (Kirk, 1994). In essence, the efficiency with which pigments absorb light decreases because they are contained within cells.

Additionally, correlation between phycocyanin model residuals and phycocyanin concentration can be explained by variation in the specific absorption coefficient in phycocyanin. Variation in the absorption per unit pigment concentration of chlorophyll *a* in living algal cells has been documented by Gitelson et al. (2007), Zimba and Gitelson (2006) Bricaud et al. (1995), and Bricaud et al. (1983). Specific absorption is dependent on the physiological conditions and structure of algal communities and varies as the size and pigment concentration of algal cells changes. Specific absorption "flattens" or decreases with increasing cell size.

Variation in phycocyanin absorption per unit of pigment concentration would be in agreement with results obtained by Simis et al. (2005). In developing their semi-empirical phycocyanin algorithm, they calculated the specific absorption coefficient of phycocyanin by dividing calculated $a_{pc}(620)$ (Equation 6) by lab measured phycocyanin

concentration. They noted high variation in the calculated phycocyanin specific absorption coefficient with a mean of 0.0095 m^2 / mg and standard deviation of 0.0033 m^2 / mg.

Phycocyanin residuals using the Gitelson R_{624} model for all of the reservoirs were highly correlated to lab measured phycocyanin concentration (Table 6): r = 0.960, 0.964, and 0.849 for Eagle Creek, Morse and Geist Reservoirs, respectively. The R_{624} only uses the absorption feature of phycocyanin in its estimates. The very strong positive correlation between this model's residuals and actual phycocyanin concentration reveal that reflectance values at approximately 620 nm do not vary consistently with increasing pigment concentration. Variation in the specific absorption by phycocyanin and/or increased scattering from algal cells walls relative to phycocyanin absorption can explain why model residuals are correlated to actual lab measured phycocyanin concentration.

A - Morse Reservoir

y = 0.39x - 35.17
$r^2 = 0.39$

B - Morse Reservoir

y = 0.93x - 83.50
$r^2 = 0.93$
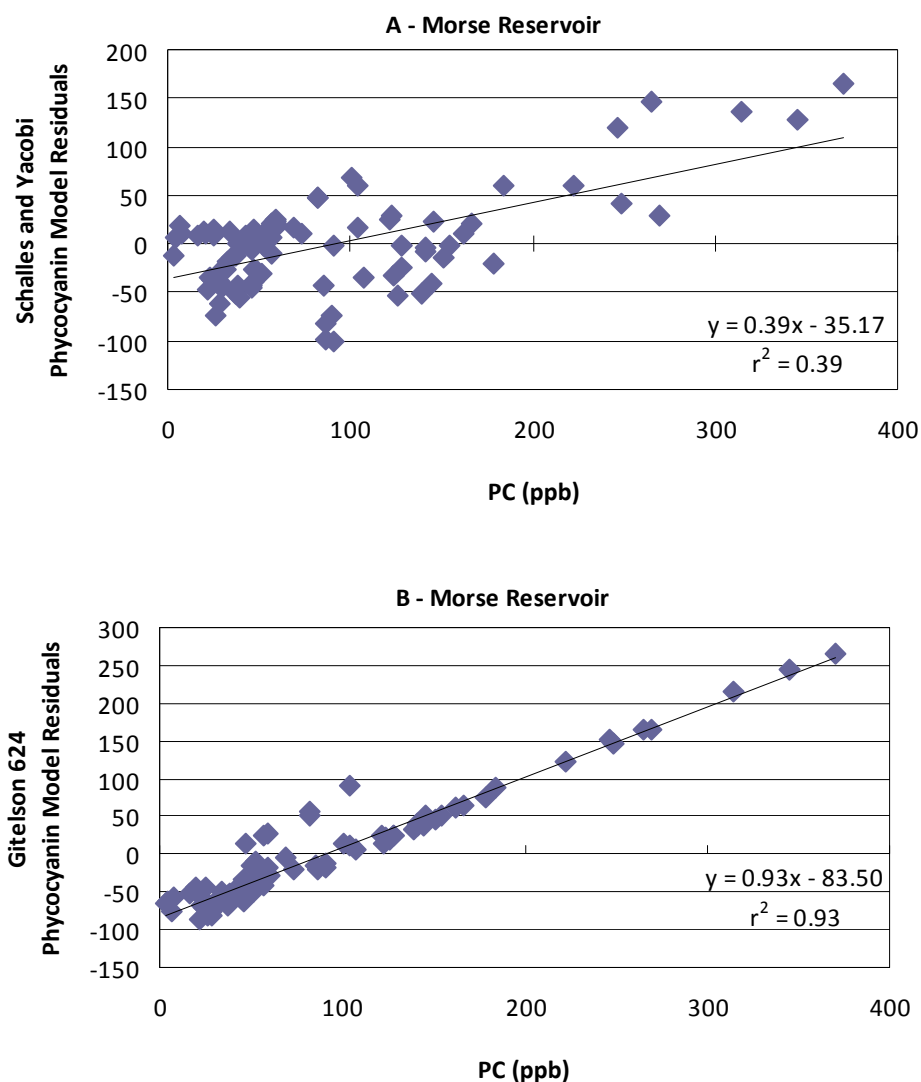
Figure 3a and b. (a) Phycocyanin residuals from the Schalles and Yacobi model and (b) Gitelson model verse measured phycocyanin concentration for Morse Reservoir.

Correlation between the phycocyanin model residuals and the other measured OACs highlighted other relationships. As with phycocyanin, higher levels of chlorophyll *a* were associated with an underestimation of phycocyanin, although this relationship was weaker across the models and reservoirs (Table 6, r < 0.74). Higher levels of chlorophyll *a* were associated with the underestimation of phycocyanin for all of the models when applied to Eagle Creek and Geist Reservoirs and for three of the five models when applied to Morse Reservoir data (Table 6).

Suspended matter had a distinctly different relationship with the residuals for Geist reservoir than with Eagle Creek and Morse Reservoirs for several of the models (Table 6). This is evident in the scatter plots of TSM versus the Schalles and Yacobi phycocyanin residuals below (Figure 4). While increasing suspended matter was associated with an overestimation of phycocyanin for Geist Reservoir, increasing suspended matter was associated with the underestimation of phycocyanin for Eagle Creek and Morse Reservoirs. This also suggests the nature of suspended matter in Eagle Creek and Morse is different than in Geist, and that this difference impacts remote sensing phycocyanin predictions.
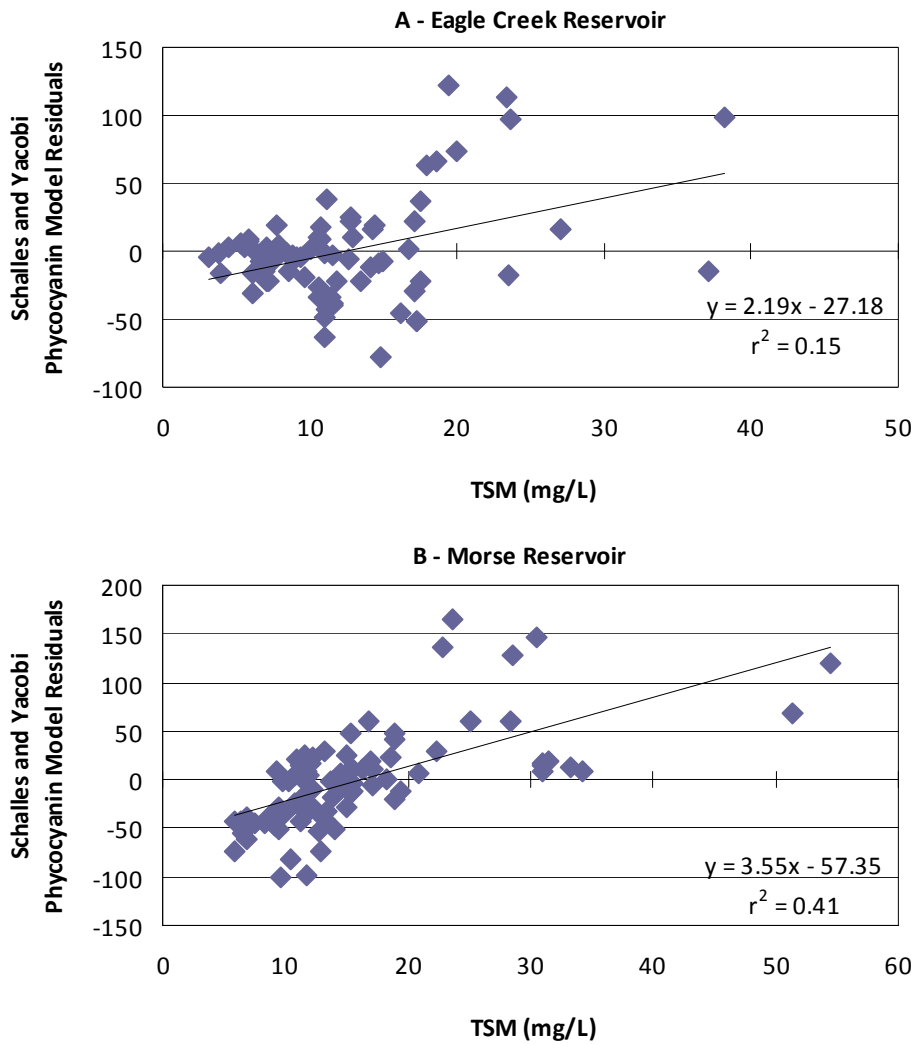
Figure 4a and b. Total suspended matter versus the Schalles and Yacobi model phycocyanin residuals for (a) Eagle Creek and (b) Morse Reservoirs.

C - Geist Reservoir

$$y = -1.2249x + 23.168$$
$$r^2 = 0.0218$$
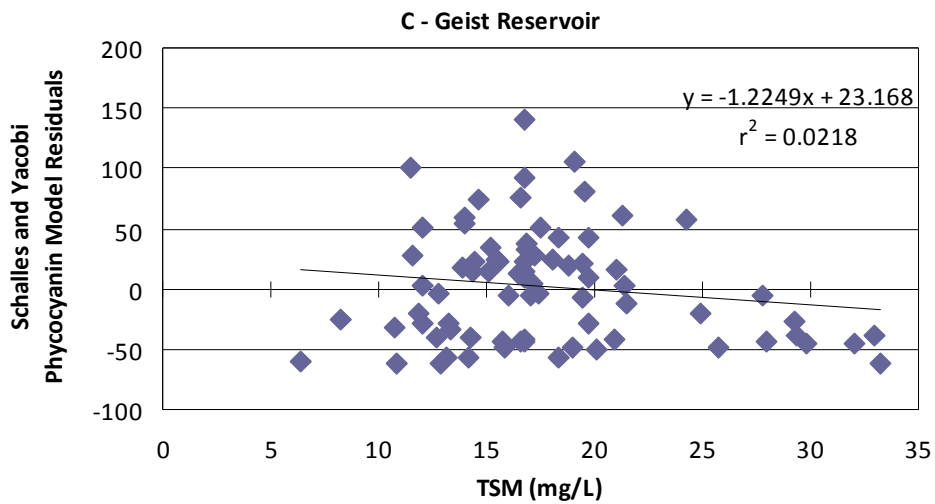
Figure 4c. Total suspended matter versus the Schalles and Yacobi model phycocyanin residuals for Geist Reservoir. Suspended matter greater than 25 mg/L was associated with the overestimation of phycocyanin, while concentrations of TSM less than 25 mg/L were both underestimated and overestimated.

Scatter plots were made of the model phycocyanin residuals versus ISM. A negative logarithmic relationship was evident for the Geist models, particularly for the Simis ratio, Schalles and Yacobi, and the Simis semi-empirical models. The relationship between ISM and the model residuals for Eagle Creek and Morse were consistently different from the Geist plots. No linear or logarithmic relationship was evident (r^2 values were 0.01 and 0.04 for Eagle Creek and Morse Reservoir, respectively). Example plots are given below (Figures 5 and 6).

A - Geist Reservoir

$$y = -33.92\mathrm{Ln}(x) + 60.58$$
$$r^2 = 0.49$$

Simis Ratio Phycocyanin Model Residual vs ISM (mg/L)

B - Geist Reservoir

$$y = -33.88\mathrm{Ln}(x) + 61.32$$
$$r^2 = 0.38$$

Schalles and Yacobi Phycocyanin Model Residual vs ISM (mg/L)
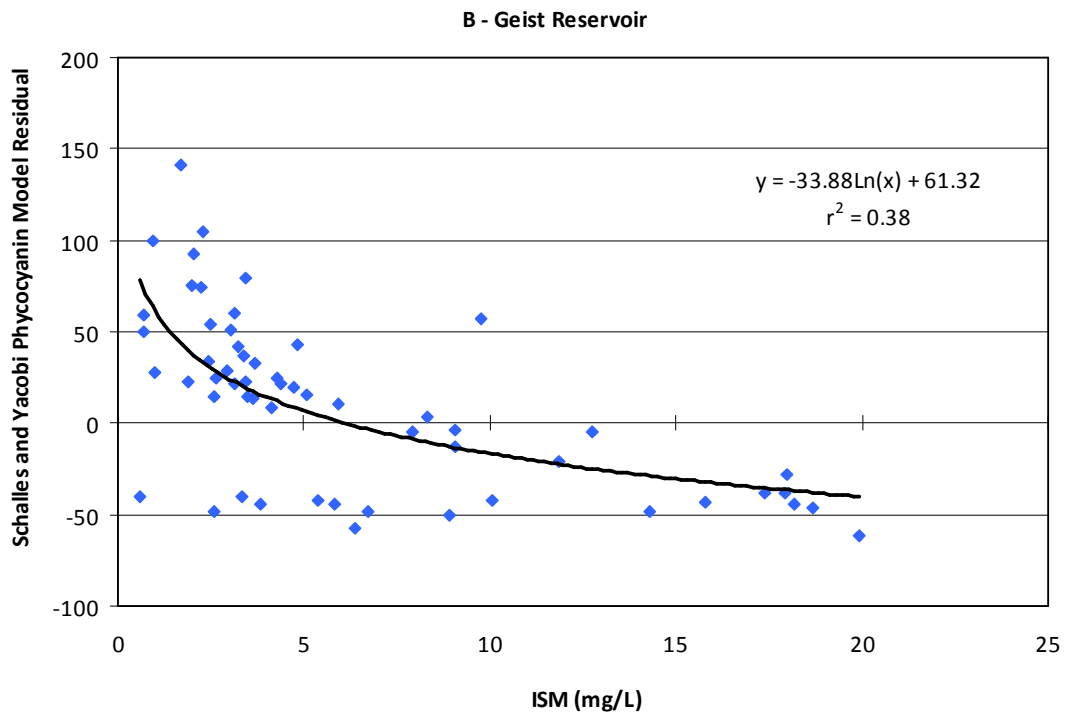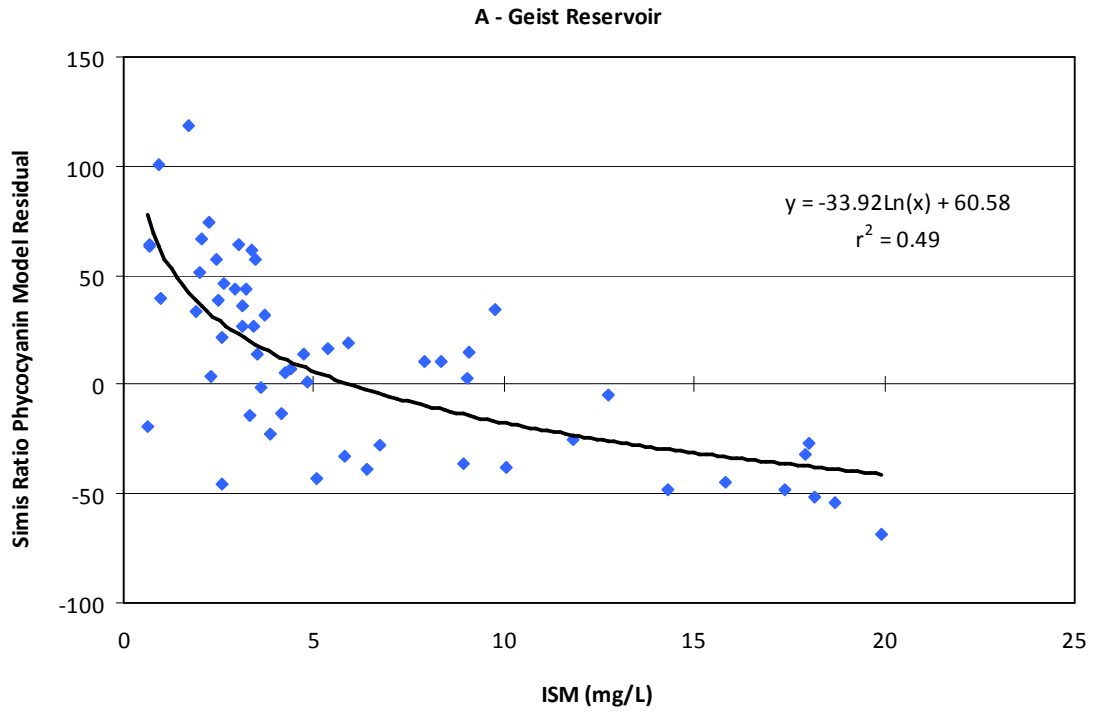
Figure 5a and b. ISM versus (a) Simis ratio and (b) Schalles and Yacobi model phycocyanin residuals for Geist Reservoir.

A - Eagle Creek Reservoir

y = -0.69x + 3.01
$r^2 = 0.01$

ISM (mg/L)

Simis Ratio Phycocyanin Model Residual

B - Morse Reservoir

y = -14.23Ln(x) + 36.98
$r^2 = 0.04$

ISM (mg/L)

Simis Ratio Phycocyanin Model Residual
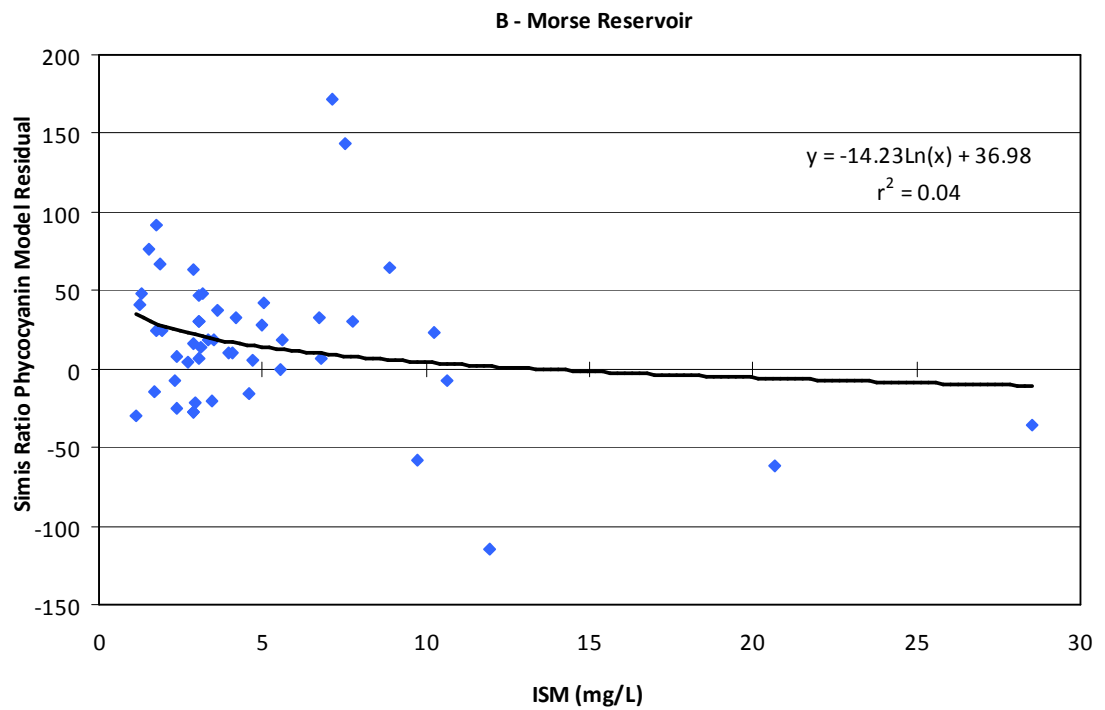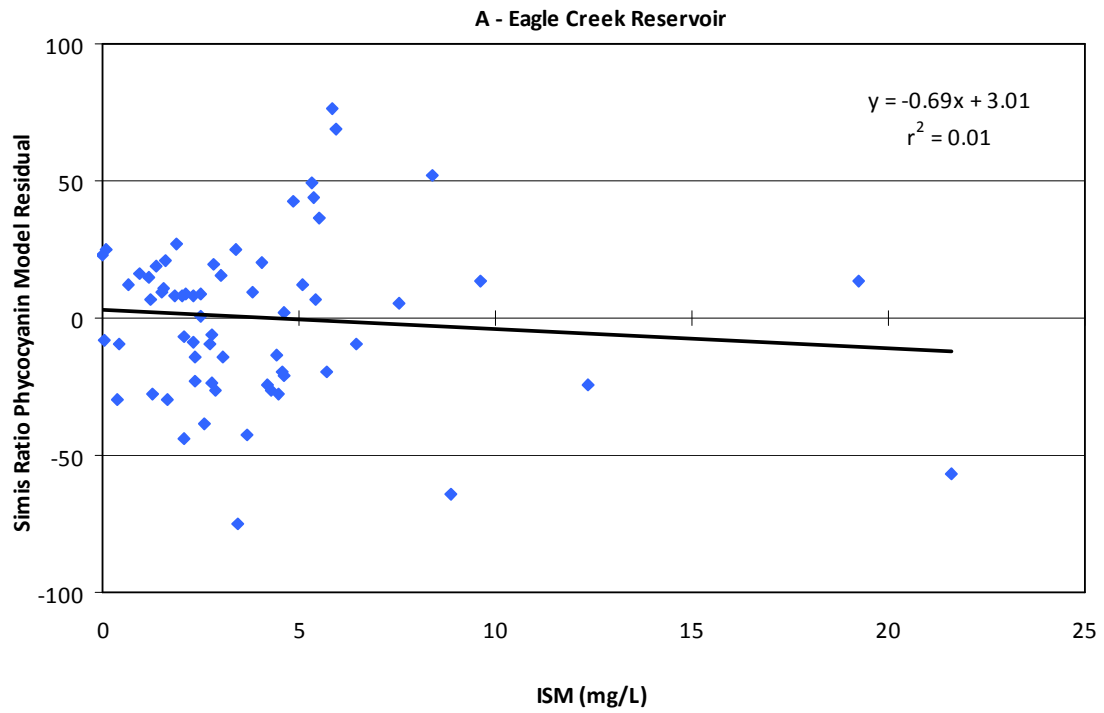
Figure 6a and b. ISM versus the Simis ratio phycocyanin residual for (a) Eagle Creek and (b) Morse Reservoirs.

Regression Residual Analysis

Phycocyanin spectral model residuals were regressed against lab measured OACs to determine the impact of each constituent while holding the impact of the other constituents constant. Results, by reservoir and model, are given in Tables 7, 8, 10, and 11. P-values significant at the 0.05 level are bolded. Positive regression coefficients are associated with the underestimation of phycocyanin, and negative regression coefficients are associated with the overestimation of phycocyanin. Results of the regressions indicate the proportion of the error in the phycocyanin model predictions that can be explained using the included OACs and which OACs are statistically significant.

Eagle Creek Reservoir Residuals

Regressions of the model residuals on Eagle Creek reservoir revealed several consistent relationships (Table 7). Dissolved organic carbon (proxy for CDOM) was a significant confounder in all of the spectral models except the R_{709} / R_{620} ratio. In the Schalles and Yacobi, Gitelson, and Dekker models, higher DOC levels were associated with the underestimation of phycocyanin. This is consistent with results reported by Schalles (2006) in which increasing levels of CDOM were shown to have a greater effect on reflectance peaks in the spectral signature of algae laden water than on absorption troughs. This could explain the observed underestimating effect for the Schalles and Yacobi and Dekker models. Both of these models utilize reflectance peaks in their phycocyanin estimations.

Phycocyanin concentration was a significant confounder in both the Gitelson and Dekker models. In both instances higher lab measured phycocyanin concentrations were associated with the underestimation of phycocyanin. This is consistent with the relationship revealed in the correlations performed in the first part of the Phase 2 analysis (Figure 2). Higher phycocyanin concentrations are consistently under predicted in the spectral models. This could be explained by variation in the specific absorption of phycocyanin and/or increased scattering by algal cells relative to increased absorption by phycocyanin.

Chlorophyll *a* was a significant confounder in three of the five models. In each of these instances, higher chlorophyll *a* values were associated with overestimation of phycocyanin. This could be due to overlapping chlorophyll *a* absorption at 620 nm. The spectral models used attribute absorption at 620 nm (lower reflectance values) to higher levels of phycocyanin, even when light at this wavelength is being absorbed by chlorophyll *a*. Thus, over prediction would increase as chlorophyll *a* concentration increases. Inorganic suspended matter was a significant confounder in just one of the spectral models (R_{650} / R_{625}). It was associated with the underestimation of phycocyanin.

Most r^2 values of the regressions were under 0.35. These regressions explained a third or less of the error in the phycocyanin spectral models using these four OACs. This indicates that the confounding factors included in the regression are not the primary source of error in the models developed for Eagle Creek Reservoir.

Table 7. Residual regression results for Eagle Creek Reservoir.

	r²	RMSE		Constant	PC	Chl *a*	ISM	DOC
R₇₀₉ / R₆₂₀	0.28	20.88	Regression Coefficient	73.503	0.091	-1.010	1.203	-14.116
			Standard Error	60.498	0.107	0.317	1.715	14.645
			Beta Coefficient		0.157	-0.677	0.129	-0.132
			p-values	0.232	0.400	**0.003**	0.487	0.341
R₆₅₀ / R₆₂₅	0.34	19.77	Regression Coefficient	-124.422	-0.087	-0.738	6.206	29.576
			Standard Error	57.270	0.101	0.300	1.623	13.863
			Beta Coefficient		-0.151	-0.499	0.671	0.280
			p-values	0.036	0.394	**0.018**	**<0.001**	**0.039**
R₆₂₄	0.90	12.65	Regression Coefficient	-250.533	0.889	-0.171	1.407	47.416
			Standard Error	36.642	0.065	0.192	1.039	8.870
			Beta Coefficient		0.933	-0.070	0.092	0.272
			p-values	<0.001	**<0.001**	0.378	0.183	**<0.001**
0.5(R₆₀₀ + R₆₄₈) − R₆₂₄	0.23	25.24	Regression Coefficient	-183.199	0.310	-0.618	0.605	43.802
			Standard Error	73.116	0.129	0.383	2.073	17.699
			Beta Coefficient		0.454	-0.354	0.055	0.351
			p-values	0.017	**0.022**	0.115	0.772	**0.018**
a_{PC}(620) / a^*_{PC}(620)	0.31	19.88	Regression Coefficient	191.819	0.046	-0.681	0.841	-44.442
			Standard Error	57.589	0.102	0.302	1.633	13.941
			Beta Coefficient		0.081	-0.469	0.093	-0.428
			p-values	0.002	0.654	**0.030**	0.609	**0.003**

Eagle Creek Reservoir, n = 44

Morse Reservoir Residuals

Relationships between the OACs and the Morse residuals mirrored relationships observed in the Eagle Creek regressions (Table 8). Chlorophyll *a* was a significant predictor of error in the three of the five models also. As in the results for Eagle Creek, chlorophyll *a* was a significant confounder in the Simis et al. ratio and the Simis et al. semi-empirical model. It was also a significant confounder in the Dekker model for Morse Reservoir. The direction of the relationship was negative: higher chlorophyll *a* concentration resulted in negative residuals (an overestimation of phycocyanin). Again, this could be due to chlorophyll *a* absorption in the 620 nm band used in the models (absorption at 620 nm is attributed to phycocyanin, when in fact it is also being absorbed by chlorophyll *a*).

Unlike Eagle Creek, phycocyanin concentration was significant in the residual regressions for every spectral model applied to Morse Reservoir samples. The direction of the relationship in each case was positive: higher phycocyanin concentration resulted in positive residuals (an underestimation of phycocyanin). This is consistent with the results observed in the exploratory bivariate correlations. Increased underestimation of pigment concentration occurred as measured pigment concentration increased. This could be explained by variation in the specific absorption of phycocyanin and/or increased scattering by algal cells relative to increased absorption by phycocyanin.

r^2 values for the regression of the residuals for Morse Reservoir were higher than those obtained by Eagle Creek. The R_{709} / R_{620} model had the lowest r^2 value ($r^2 = 0.28$) while the r^2 values for the other models ranged from 0.67 to 0.90. Excluding the R_{709} / R_{620} model, the regressions explain the majority of the error in phycocyanin predictions for Morse Reservoir using the included OACs.

Table 8. Residual regression results for Morse Reservoir.

	r²	RMSE		Constant	PC	Chl *a*	ISM	DOC
			Regression Coefficient	167.989	0.677	-1.153	-9.044	-31.124
	0.28	20.88	Standard Error	124.716	0.116	0.540	6.101	32.246
			Beta Coefficient		1.370	-0.686	-0.418	-0.160
			p-values	0.197	**<0.001**	**0.049**	0.158	0.349
			Regression Coefficient	107.087	0.379	-0.671	9.944	-32.832
R₆₅₀ / R₆₂₅	0.67	24.22	Standard Error	119.324	0.111	0.517	5.838	30.852
			Beta Coefficient		0.865	-0.451	0.519	-0.190
			p-values	0.383	**0.004**	0.212	0.108	0.303
			Regression Coefficient	108.132	0.818	0.416	0.474	-46.740
R₆₂₄	0.90	27.53	Standard Error	135.638	0.126	0.587	6.636	35.070
			Beta Coefficient		0.902	0.135	0.012	-0.131
			p-values	0.437	**<0.001**	0.489	0.944	0.201
			Regression Coefficient	-97.644	0.992	-1.693	7.474	11.708
0.5(R₆₀₀ + R₆₄₈) − R₆₂₄	0.87	29.63	Standard Error	145.970	0.136	0.632	7.141	37.742
			Beta Coefficient		1.182	-0.593	0.204	0.035
			p-values	0.513	**<0.001**	**0.016**	0.311	0.760
			Regression Coefficient	5.855	0.889	-2.759	-0.296	9.534
***a*PC(620) / *a**PC(620)**	0.88	21.44	Standard Error	105.622	0.098	0.457	5.167	27.309
			Beta Coefficient		1.388	-1.267	-0.011	0.038
			p-values	0.956	**<0.001**	**<0.001**	0.955	0.732

Morse Reservoir, n = 21

Maximum phycocyanin concentrations were significantly higher in Morse Reservoir than in Eagle Creek and Geist Reservoirs (Table 9) for the entire 2006 dataset. In the subset of samples used in the regressions (n = 21) phycocyanin was also significantly higher than the subset of samples for Eagle Creek and Geist Reservoirs. A second set of regressions were run on the Phase 1 models residuals for Morse Reservoir excluding the outlying sample that had a lab measured phycocyanin concentration greater than 300 ppb (371.0 ppb). It was hypothesized that by excluding this sample, relationships existing between the other OACs and the model residuals would be identified.

Table 9. Comparison of measured phycocyanin concentration across sampled reservoirs for the entire 2006 data set and the Phase 2 subset.

Phycocyanin Concentration (ppb)						
	Entire 2006 Data Set			Phase 2 Data Subset		
	Mean	Median	Maximum	Mean	Median	Maximum
Eagle Creek	55.3	28	243.3	38.1	27.8	137.6
Morse	88.9	58.3	371.0	104.9	59.6	371.0
Geist	86.2	87.1	210.2	106.8	108.2	208.3

Results for the second set of regressions are given in Table 10. In this set of regressions, phycocyanin concentration was still a significant predictor for the Gitelson, Dekker, and Simis et al. semi-empirical models. Chlorophyll a remained a significant confounder in the Simis et al. semi-empirical model, though it was no longer a significant confounder in the Simis et al. ratio and the Dekker model. Dissolved organic carbon remained statistically insignificant for all of the models. r^2 values for this set of regressions dropped from the original set, excluding the Gitelson R_{624} and Simis et al. ratio. For the Simis et al. ratio, ISM became statistically significant and r^2 value increased from 0.28 to 0.68.

Table 10. Residual regression results for Morse Reservoir, excluding sample with phycocyanin concentration greater than 300 ppb.

	r^2	RMSE		Constant	PC	Chl a	ISM	DOC
						Morse Reservoir, n = 20		
R_{709} / R_{620}	0.69	18.11	Regression Coefficient	60.498	0.221	0.035	-15.981	0.005
			Standard Error	93.114	0.140	0.486	4.691	24.325
			Beta Coefficient		0.487	0.031	-1.046	<0.001
			p-values	0.526	0.135	0.943	**0.004**	1.000
R_{650} / R_{625}	0.47	17.38	Regression Coefficient	4.508	-0.056	0.463	3.324	-3.127
			Standard Error	89.338	0.134	0.466	4.501	23.339
			Beta Coefficient		-0.165	0.541	0.294	-0.032
			p-values	0.960	0.684	0.337	0.472	0.895
R_{624}	0.90	27.53	Regression Coefficient	108.132	0.818	0.416	0.474	-46.740
			Standard Error	135.638	0.126	0.587	6.636	35.070
			Beta Coefficient		0.902	0.135	0.012	-0.131
			p-values	0.437	**<0.001**	0.489	0.944	0.201
$0.5(R_{600} + R_{648}) - R_{624}$	0.69	30.34	Regression Coefficient	-120.713	0.895	-1.438	5.985	18.388
			Standard Error	155.959	0.235	0.814	7.858	40.742
			Beta Coefficient		1.172	-0.742	0.233	0.083
			p-values	0.451	**0.002**	0.098	0.458	0.658
$a_{PC}(620) / a*_{PC}(620)$	0.81	20.9	Regression Coefficient	-35.927	0.712	-2.297	-2.993	21.634
			Standard Error	107.431	0.162	0.561	5.413	28.065
			Beta Coefficient		1.047	-1.331	-0.131	0.110
			p-values	0.743	**0.001**	**0.001**	0.588	0.453

Geist Reservoir Residuals

The regressions on the Geist Reservoir model residuals revealed relationships not present in the other two reservoirs (Table 11). Noteworthy of the Geist Reservoir regressions are the high r^2 values. These models explain 84% to 95% of the variation in the phycocyanin model residuals on the tested sample set. Geist marks a unique case different from Eagle Creek and Morse Reservoirs, where the four measured OACs are the primary source of model error. This is relevant considering the poor performance of the original spectral models on Geist Reservoir.

Like the other reservoirs, phycocyanin was a significant confounder in two of the five models. Higher phycocyanin concentrations were associated with the underestimation of pigment concentration. This could be explained by variation in the specific absorption of phycocyanin and/or increased scattering by algal cells relative to increased absorption by phycocyanin. Chlorophyll *a* was a significant confounder in two of the models, demonstrating an inverse relationship. Higher chlorophyll *a* concentrations were related to negative residuals and the overestimation of phycocyanin.

Inorganic suspended matter was a significant confounder in four of the five spectral models. The direction of this relationship varied. In the models that used band ratios with reflectance peaks as numerators, the Simis et al. models (ratio and semi-empirical) and the Schalles and Yacobi model, higher ISM concentrations were related to overestimating phycocyanin. In the Gitelson and Dekker models higher ISM values were related to underestimating phycocyanin.

Table 11. Residual regression results for Geist Reservoir.

Geist Reservoir, n = 18								
	r²	RMSE		Constant	PC	Chl *a*	ISM*	DOC
R_{709} / R_{620}	0.84	16.33	Regression Coefficient	215.859	0.146	-0.573	-109.623	-26.026
			Standard Error	68.224	0.177	0.184	25.873	16.408
			Beta Coefficient		0.214	-0.460	-0.983	-0.228
			p-values	**0.007**	0.426	**0.008**	**0.001**	0.137
R_{650} / R_{625}	0.85	19.23	Regression Coefficient	-32.260	0.253	0.634	-50.848	3.385
			Standard Error	81.223	0.211	0.219	30.802	19.535
			Beta Coefficient		0.292	0.402	-0.360	0.023
			p-values	0.698	0.253	**0.012**	0.123	0.865
R_{624}	0.85	17.82	Regression Coefficient	-188.816	1.157	0.020	95.287	3.958
			Standard Error	75.251	0.196	0.203	28.538	18.098
			Beta Coefficient		1.451	0.014	0.731	0.030
			p-values	0.026	**<0.001**	0.922	**0.005**	0.830
$0.5(R_{600} + R_{648}) - R_{624}$	0.95	11.5	Regression Coefficient	-208.172	1.516	-0.266	116.082	-0.562
			Standard Error	48.590	0.126	0.131	18.427	11.686
			Beta Coefficient		1.661	-0.160	0.777	-0.004
			p-values	0.001	**<0.001**	0.063	**<0.001**	0.962
$a_{PC}(620)$ / $a*_{PC}(620)$	0.84	16.33	Regression Coefficient	195.111	0.140	-0.262	-110.384	-25.883
			Standard Error	68.968	0.179	0.186	26.155	16.587
			Beta Coefficient		0.195	-0.201	-0.942	-0.216
			p-values	0.014	0.449	0.181	**0.001**	0.143

*log taken

Phase 2 Summary

The following is a table summarizing the results of the exploratory and regression residual analysis.

Table 12. Phase 2 summary.

The tested empirical and semi-empirical phycocyanin spectral models work well when:	
measured OACs are a function of phytoplankton (OACs co-vary)	
The tested empirical and semi-empirical phycocyanin spectral models do not work well when:	
Condition	*Impact*
non-covarying ISM	overestimates phycocyanin when using band ratios that use reflectance peaks
very high phycocyanin concentrations	underestimates phycocyanin as lab measured concentration increases
non-covarying high chlorophyll *a* concentration	overestimates phycocyanin as chlorophyll *a* concentration increases

Phase 3: Inclusion of confounding variables into new spectral models

Significant confounding OACs can be incorporated into the phycocyanin spectral models to account for their influence. As an example, combining ISM as an additional independent variable with the Simis ratio model for Geist Reservoir, the r^2 for phycocyanin concentration increases from 0.54 to 0.93 (Table 13, Figure 7 below). This is nearly a twofold increase from the original model applied to the same sample subset.

Table 13. Incorporating ISM as a control with the Simis ratio spectral model to predict phycocyanin for Geist Reservoir applied to Phase 2 samples.

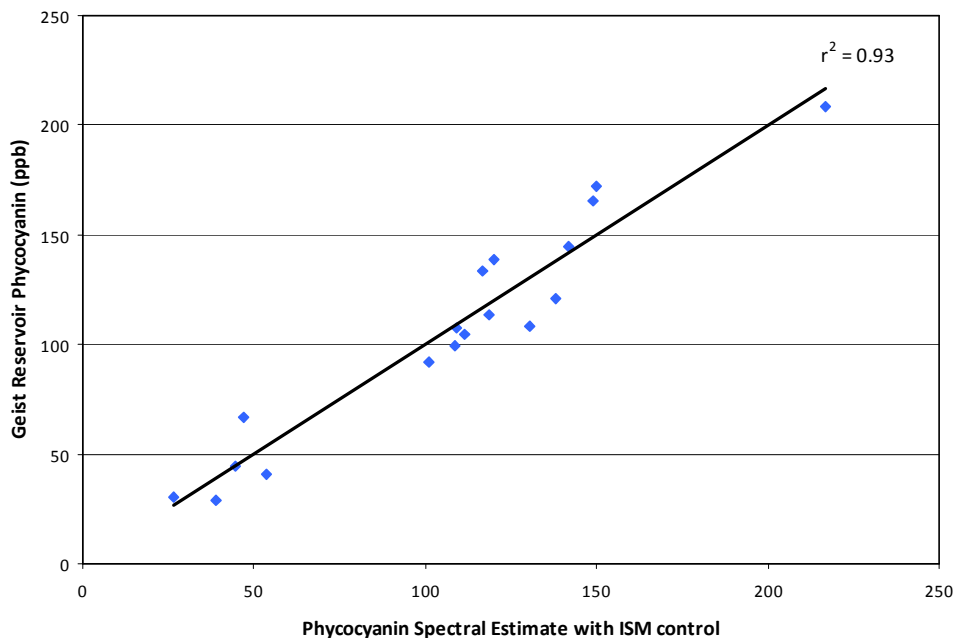|	Geist Reservoir, Simis Ratio PC Estimate Controlling for ISM			Geist Reservoir, Simis Ratio PC Estimate		
r^2	0.93			0.54		
Standard Error	14.52			35.47		
Observations	18			18		
	Regression Coefficient	Standard Error	p-value	Regression Coefficient	Standard Error	p-value
Constant	-66.918	32.045	0.054	-193.28	70.303	0.014
Simis Ratio	182.394	25.45	**<0.001**	253.821	59.043	**0.001**
ISM	-7.409	0.826	**<0.001**	-	-	-

Figure 7. Spectral phycocyanin estimate with ISM control for Geist Reservoir.

The purpose of Phase 3 was to evaluate the potential for improved phycocyanin estimates by attempting to spectrally estimate and account for confounding constituents identified in Phase 2. Previously published remote sensing algorithms developed to estimate the confounding constituents are combined with the phycocyanin algorithms used in Phase 1.

The success of this technique is limited by the ability to spectrally estimate the confounders. Suspended matter is particularly challenging because of its diversity in composition, size, and concentration. Several authors report difficulty remotely estimating the concentration of suspended sediment and also suggest there is no universal algorithm to detect this constituent's concentration (Warrick et al., 2004; Gin et al., 2003). Spectral ratios used to estimate chlorophyll *a*, ISM, and CDOM are given below in Table 14. Results by reservoir follow.

Table 14. Spectral ratios used to estimate and control for confounding OACs.

OAC	Spectral Ratio	Source
Chlorophyll *a*	$R_{max \lambda (700 - 710)} / R_{min \lambda (665 - 675)}$	Modified from Gitelson et al., 2000
ISM	R_{560} / R_{620}	Gitelson et al., 1993
CDOM	R_{480} / R_{520}	Gitelson et al., 1993

Multivariate Phycocyanin Models: Eagle Creek Reservoir

Multivariate spectral models to predict phycocyanin developed for Eagle Creek Reservoir are given in Table 15. In Eagle Creek Reservoir, the only model that had a significant improvement in r^2 values when controlling for significant confounders was the Schalles and Yacobi ratio. The r^2 value increased from 0.70 in Phase 1 to 0.83. Standard error decreased from 37.25 ppb to 17.31 ppb. For this particular model in the Phase 2 regressions, chlorophyll *a*, ISM, and DOC were all significant confounders.

In the model developed to control for these confounders though, only the spectral ratios used to control for chlorophyll *a* and DOC were statistically significant at the 0.05 level. The ISM ratio (R_{560} / R_{620}) was statistically insignificant. A new model excluding the insignificant ISM variable (Table 16, Figure 8) was developed and is tested on the validation set in Phase 4. The r^2 values and RMSE remain high for the new model, 0.83 and 17.12 ppb, respectively.

There are several reasons OACs identified as statistically significant in the analysis of phycocyanin residuals in Phase 2 become statistically insignificant when incorporated into a multivariate spectral model to predict phycocyanin. The variables incorporated in Phase 3 are spectral estimates of the confounders, not the actual ground-truth measurements of the confounders that were used in Phase 2. It is likely these spectral variables are limited in their ability to model each constituent, just as the spectral algorithms in Phase 1 were limited in their ability predict phycocyanin concentration. The success of accounting for a significant confounder is confined by the ability to spectrally estimate it with this approach.

Additionally, analysis of the residuals and the prediction of phycocyanin involve modeling different phenomena. Though residuals are calculated using lab measured phycocyanin concentration (the variables are related) the models are analyzing different dependent variables.

Table 15. Phycocyanin models with additional spectral variables for Eagle Creek Reservoir.

r^2	Standard Error		Constant	PC spectral estimate	Chl a (R_{705}/R_{670})	ISM (R_{560}/R_{620})	CDOM (R_{480}/R_{520})
				R_{709} / R_{620}			
0.80	18.50	Regression Coefficient	-129.320	159.387	4.946	not significant in Phase 2	not significant in Phase 2
		Standard Error	13.732	30.699	24.046		
		Beta Coefficient		0.862	0.034		
		p-value	<0.001	**<0.001**	0.838		
				R_{650} / R_{625}			
0.83	17.31	Regression Coefficient	-681.153	441.847	82.101	8.053	180.751
		Standard Error	100.653	108.161	29.362	23.483	82.013
		Beta Coefficient		0.626	0.567	0.045	0.392
		p-value	<0.001	**<0.001**	**0.008**	0.733	**0.033**
				R_{624}			
0.29	34.60	Regression Coefficient	246.594	386.702	not significant in Phase 2	not significant in Phase 2	-278.494
		Standard Error	56.977	694.433			84.569
		Beta Coefficient		0.102			-0.604
		p-value	<0.001	0.581			**0.002**
				$0.5(R_{600} + R_{648}) - R_{624}$			
0.62	25.14	Regression Coefficient	6.219	35044.708	not significant in Phase 2	not significant in Phase 2	-35.665
		Standard Error	50.221	5743.251			55.954
		Beta Coefficient		0.740			-0.077
		p-value	0.902	**<0.001**			0.527
				$a_{PC}(620) / a*_{PC}(620)$			
0.82	17.35	Regression Coefficient	49.630	2.228	not significant in Phase 2	not significant in Phase 2	-91.821
		Standard Error	28.765	0.201			33.453
		Beta Coefficient		0.805			-0.199
		p-value	0.092	**<0.001**			**0.009**

Table 16. New phycocyanin model for Eagle Creek Reservoir
with significant spectral variables.

r²	0.83			
Standard Error	17.12			
Observations	44			
	Regression Coefficient	Standard Error	Beta Coefficient	p-value
Constant	-665.716	89.026		<0.001
PC (R_{650} / R_{625})	458.312	95.844	0.649	**<0.001**
Chl a (R_{705}/R_{670})	78.109	26.657	0.539	**0.006**
CDOM (R_{480}/R_{520})	160.361	55.859	0.348	**0.007**
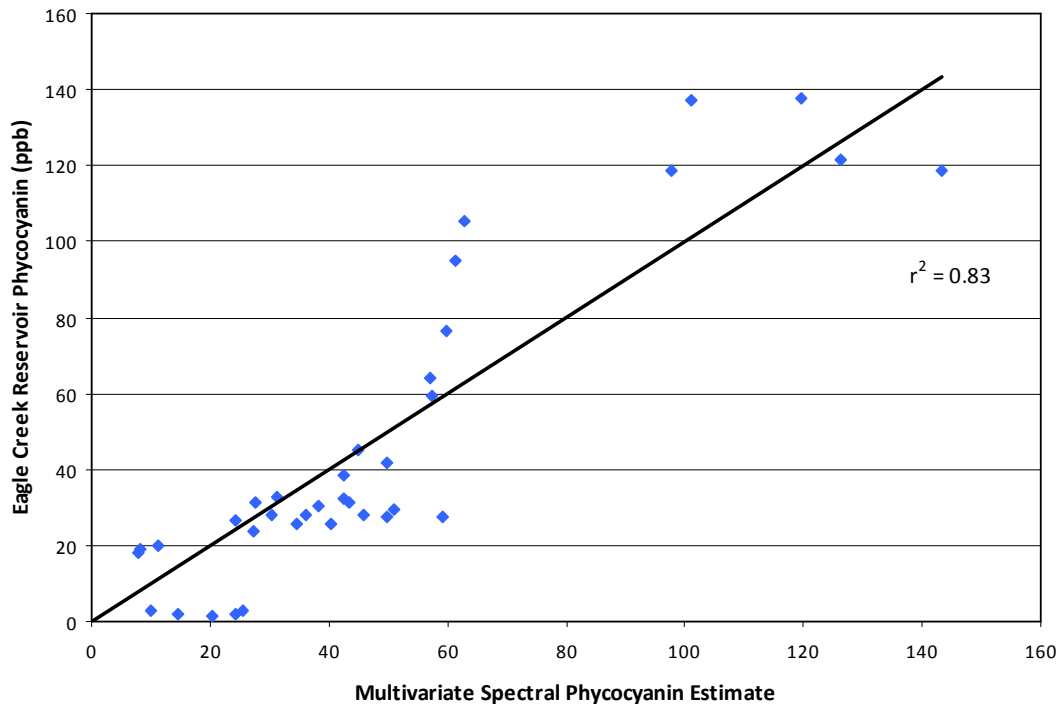
Figure 8. Multivariate phycocyanin spectral estimate for Eagle Creek Reservoir training
set versus lab measured phycocyanin concentration.

Multivariate Phycocyanin Model: Morse Reservoir

The first regressions performed on the Morse Reservoir residuals revealed high
phycocyanin values controlled model error (Table 7). Exclusion of the sample with the
highest phycocyanin concentration identified ISM as a significant confounder in the
Simis et al. (2005) ratio. A new model utilizing the R_{709} / R_{620} ratio and including a

spectral ratio to account for the influence of ISM is shown in Table 17. The coefficient of determination increased from 0.71 using only the Simis et al. ratio to 0.92 when the ISM ratio was included. RMSE decreased from 42.90 to 18.45 ppb.

Table 17. New multivariate phycocyanin model for Morse Reservoir.

| r^2	0.92			
Standard Error	18.45			
Observations	20			
	Regression Coefficient	Standard Error	Beta Coefficient	p-value
Constant	-191.220	22.487		<0.001
PC (R_{709} / R_{620})	167.064	15.803	0.786	**<0.001**
ISM (R_{560}/R_{620})	64.101	15.394	0.310	**0.001**
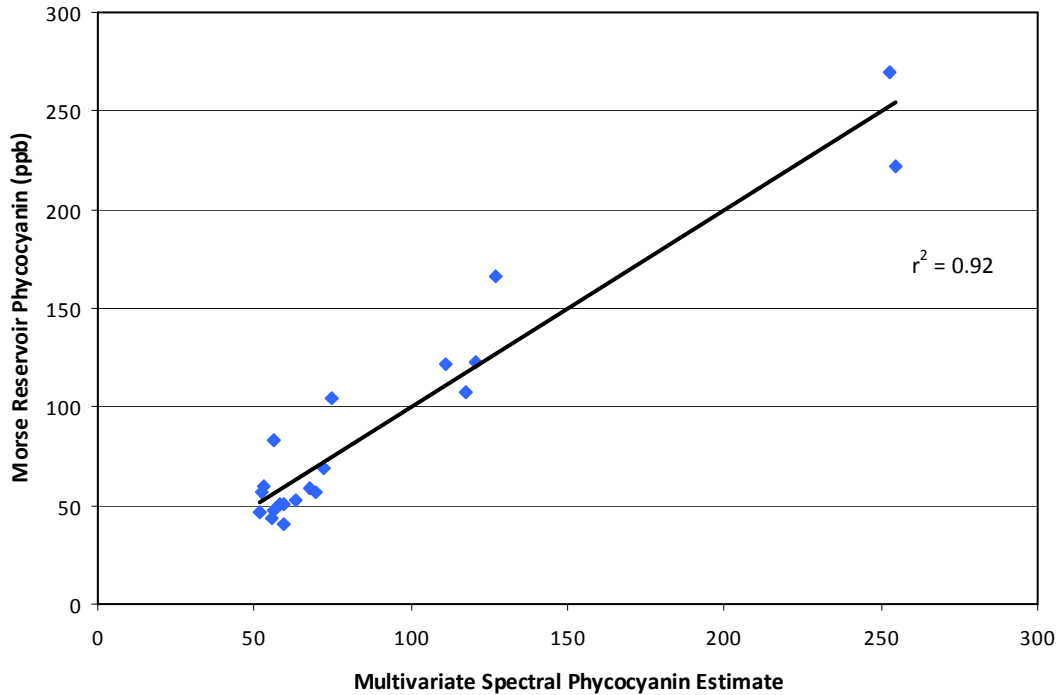
Figure 9. Multivariate phycocyanin spectral estimate for Morse Reservoir training set versus lab measured phycocyanin concentration.

Multivariate Phycocyanin Model: Geist Reservoir

Multivariate spectral models to predict phycocyanin developed for Eagle Creek Reservoir are given in Table 18. Only the ISM variables incorporated into the Simis et al. (2005) algorithms were statistically significant at the 0.05 level. The spectral variable included to control for chlorophyll *a* (identified as a significant confounder in phase 2) was not statistically significant. A new model excluding this variable but including the ISM ratio is shown in Table 19. This model is validated on a sample set in phase 4.

Table 18. Phycocyanin models with spectral variables for Geist Reservoir.

r^2	Standard Error		Constant	PC spectral estimate	Chl a (R_{705}/R_{670})	ISM (R_{560}/R_{620})
				R_{709} / R_{620}		
0.81	24.32	Regression Coefficient	-417.040	331.389	-58.790	155.373
		Standard Error	77.542	76.433	52.558	41.469
		Beta Coefficient		0.956	-0.252	0.462
		p-value	0.000	**0.001**	0.282	**0.002**
				R_{650} / R_{625}		
0.39	42.02	Regression Coefficient	-748.190	695.099	87.835	not significant in Phase 2
		Standard Error	336.228	328.367	47.945	
		Beta Coefficient		0.434	0.376	
		p-value	0.042	0.051	0.087	
				R_{624}		
0.37	42.62	Regression Coefficient	126.704	-2223.001	not significant in Phase 2	23.982
		Standard Error	169.790	1228.544		103.150
		Beta Coefficient		-0.555		0.071
		p-value	0.467	0.090		0.819
				$0.5(R_{600} + R_{648}) - R_{624}$		
0.29	45.26	Regression Coefficient	-26.172	-21818.039	not significant in Phase 2	128.628
		Standard Error	137.098	19868.437		79.496
		Beta Coefficient		-0.260		0.383
		p-value	0.851	0.289		0.126
				$a_{PC}(620) / a^*_{PC}(620)$		
0.77	25.82	Regression Coefficient	-270.988	3.173	not significant in Phase 2	178.117
		Standard Error	64.365	0.538		41.756
		Beta Coefficient		0.732		0.530
		p-value	0.001	**<0.001**		**0.001**

Table 19. New multivariate phycocyanin model for Geist Reservoir.

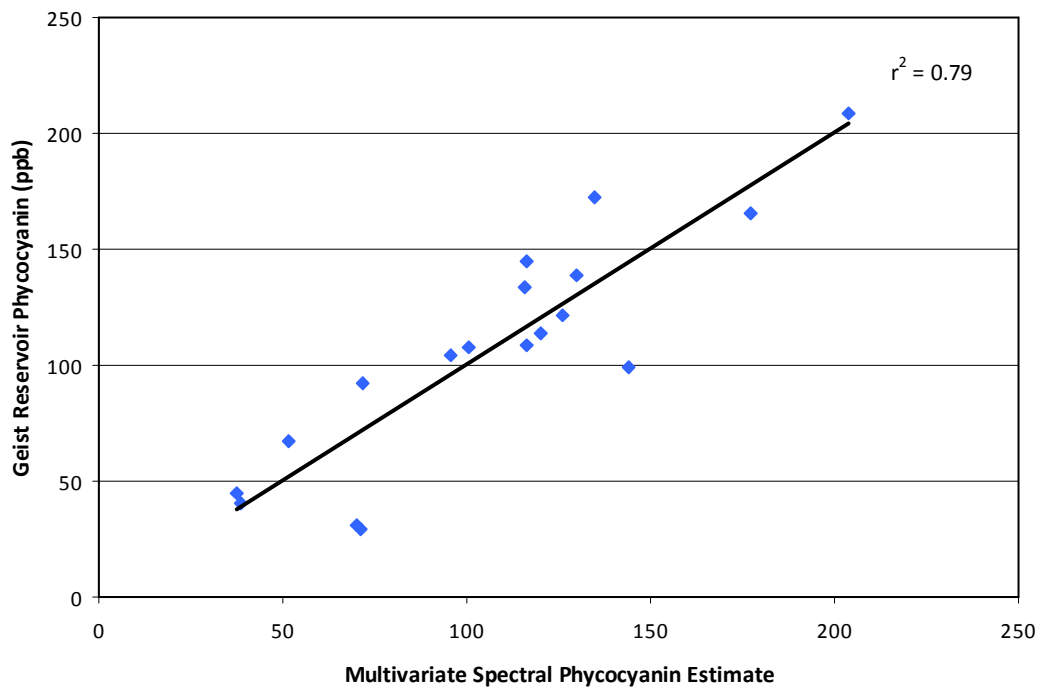|	Regression Coefficient	Standard Error	Beta Coefficient	p-value
r^2	0.792			
Standard Error	24.52			
Observations	18			
Constant	-440.496	75.275		<0.001
PC (R_{709} / R_{620})	258.874	40.826	0.747	**<0.001**
ISM (R_{560}/R_{620})	170.276	39.598	0.506	**0.001**

Figure 10. Multivariate phycocyanin spectral estimate for Geist Reservoir training set versus lab measured phycocyanin concentration.

Multivariate Phycocyanin Model: Aggregated data set

Because it consistently performs well, the Simis ratio was combined with spectral variables for the three additional OACs and applied to an aggregated data set. Samples analyzed in the regressions on the residuals were used, excluding the sample with a phycocyanin concentration greater than 300 ppb. Model results are shown in Table 20. Because the variable to control for the influence of chlorophyll *a* was not statistically significant, a new model was developed excluding this spectral variable (Table 21, Figure 11).

Table 20. Model trained on aggregated data set, including
spectral variables for all measured OACs.

r^2	0.832			
Standard Error	24.03			
Observations	82			
	Regression Coefficient	Standard Error	Beta Coefficient	p-value
Constant	-547.525	67.542		<0.001
PC (R_{709} / R_{620})	165.625	30.802	0.681	**<0.001**
Chl a (R_{705} / R_{670})	50.229	31.800	0.246	0.118
ISM (R_{560} / R_{620})	80.805	14.530	0.326	**<0.001**
CDOM (R_{480} / R_{520})	314.623	59.767	0.427	**<0.001**

Table 21. Model trained on aggregated data set, including
spectral variables for OACs that were statistically significant.

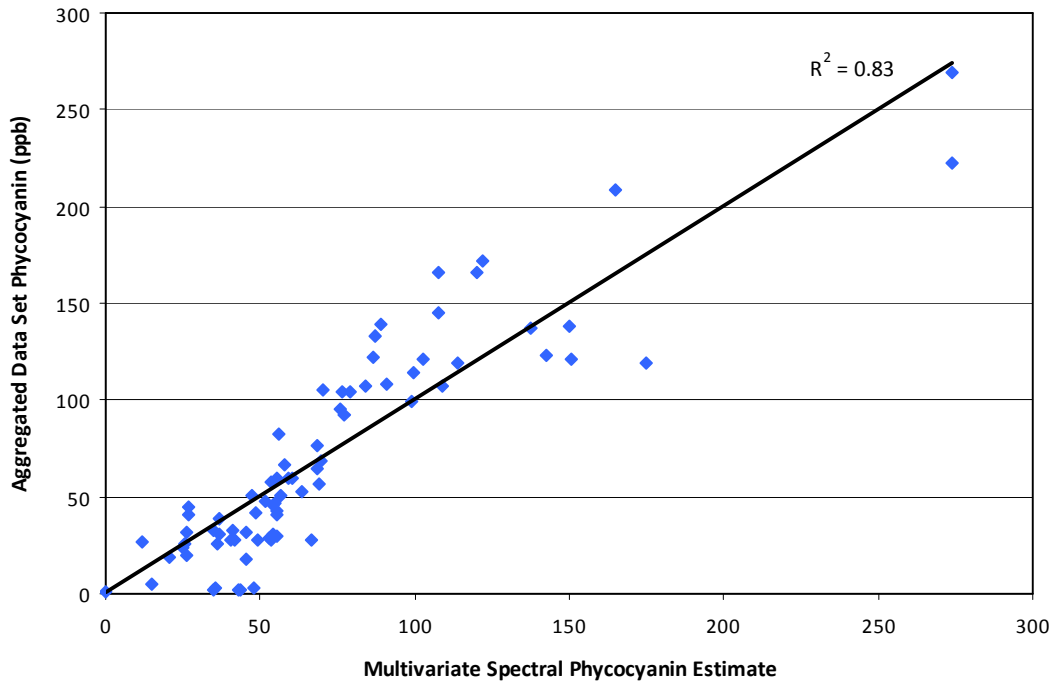| r^2	0.827			
Standard Error	24.26			
Observations	82			
	Regression Coefficient	Standard Error	Beta Coefficient	p-value
Constant	-479.078	52.303		<0.001
PC (R_{709} / R_{620})	210.089	12.624	0.864	**<0.001**
ISM (R_{560} / R_{620})	82.532	14.627	0.333	**<0.001**
CDOM (R_{480} / R_{520})	249.717	43.814	0.339	**<0.001**

Figure 11. Multivariate phycocyanin spectral estimate for the aggregated training set versus lab measured phycocyanin concentration.

Phase 4: Validation Algorithm Set

To evaluate the accuracy and transferability of the multivariate phycocyanin spectra models, models developed in Phase 3 are applied to samples that were not used in the model's development. Samples used to "validate" the models are the samples used in Phase 1 that were not used in Phase 2 (samples that had phycocyanin lab measurements and spectra, but did not have lab measurements for the other OACs. Samples that had phycocyanin concentrations greater than 300 ppb were also excluded (n = 3). Sample sizes for each reservoir are the following:

Table 22. Number of samples used in validation.

Reservoir	*Validation Sample Size*
Eagle Creek	37
Morse	63
Geist	62
Aggregated	162

Eagle Creek Model Validation

The model developed in Phase 3 for Eagle Creek Reservoir used the Schalles and Yacobi spectral ratio in addition to incorporating spectral variables to account for the influence of chlorophyll *a* and CDOM. The model was in the form of (also see Table 10):

$$PC = -665.716 + 458.312(R_{650} / R_{625}) + 78.109(R_{705} / R_{670})$$
$$+ 160.361(R_{480} / R_{520})$$

Equation 12

Application of this model on the Eagle Creek Reservoir validation sample set (n = 37) resulted in an r^2 value of 0.78 and RMSE of 39.95 ppb.
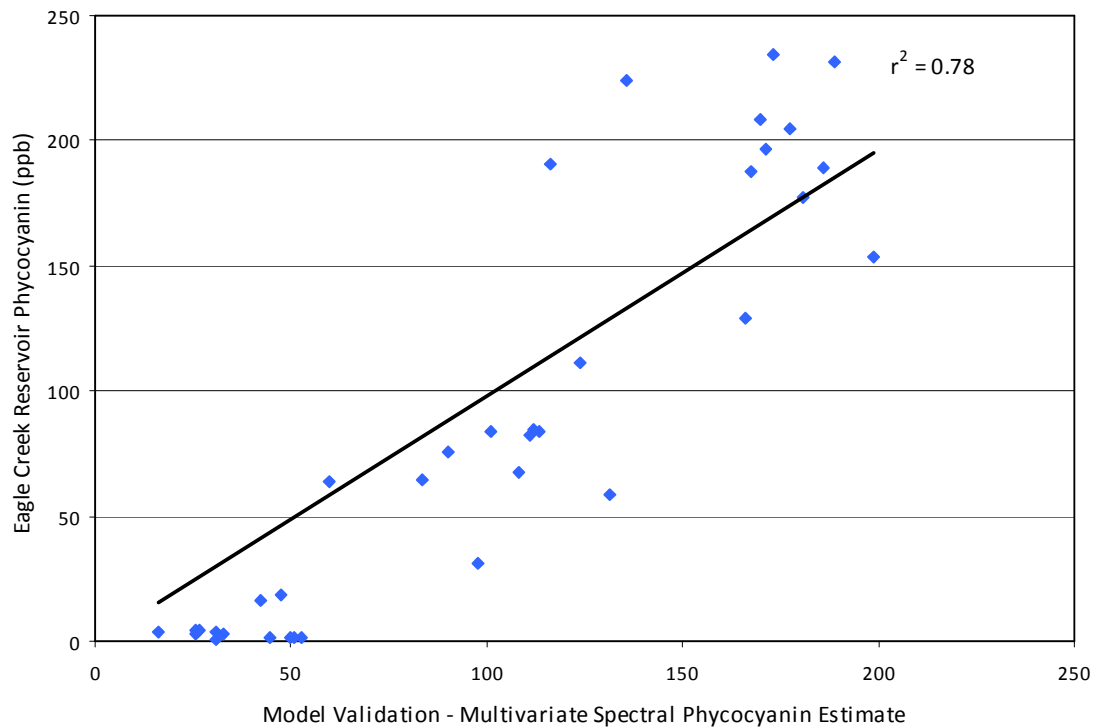

Figure 12. Validation of multivariate phycocyanin model for Eagle Creek Reservoir.

Morse Reservoir Model Validation

The model developed in Phase 3 for Morse Reservoir used the Simis ratio in addition to a variable to control for ISM. The model equation (also see Table 17) was:

$$PC = -191.220 + 167.064(R_{709} / R_{620}) + 64.101(R_{560} / R_{620})$$

Equation 13

Applying this model to the remaining Morse Reservoir data set (n = 63) resulted in an r^2 value of 0.75 and RMSE 41.31 ppb.
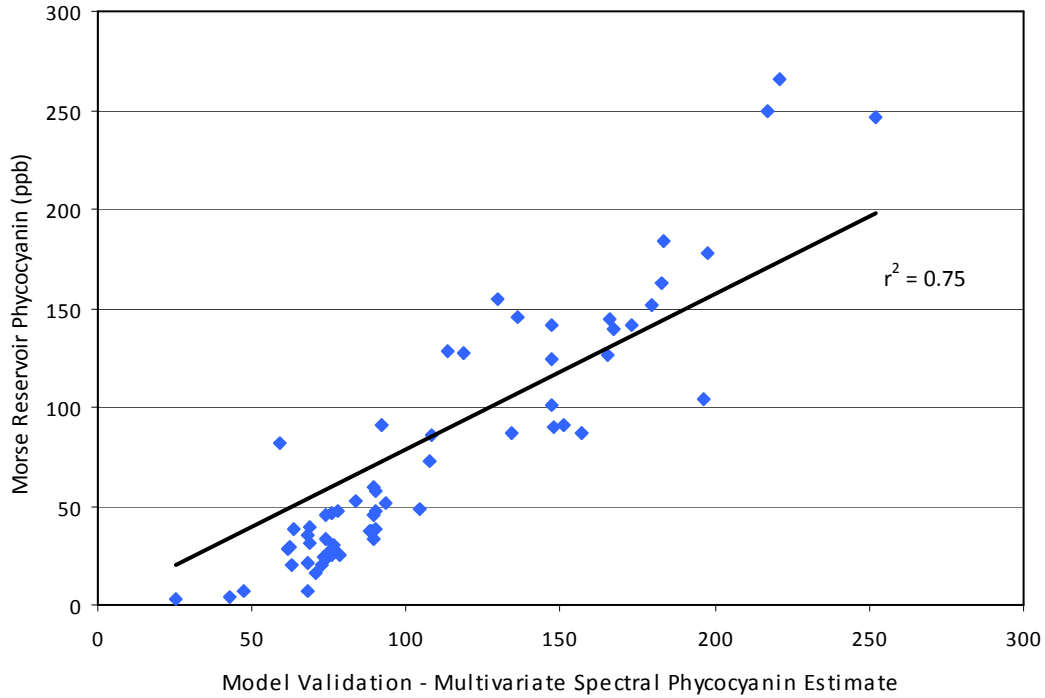
Figure 13. Validation of multivariate phycocyanin model for Morse Reservoir.

Geist Reservoir Model Validation

The model developed in Phase 3 for Geist Reservoir used the Simis ratio in addition to a spectral ISM variable. The model (also see Table 19) was in the form of:

$$PC = -440.496 + 258.874(R_{709} / R_{620}) + 170.276(R_{560} / R_{620})$$ Equation 14

The Geist Reservoir validation (n = 62) had the poorest performance of the three reservoirs. Applying the model developed in phase three resulted in an r^2 value of 0.16 and a high RMSE of 54.54 ppb.

Figure 14. Multivariate phycocyanin spectral estimate versus lab measured phycocyanin concentration for Geist Reservoir.

Aggregated Data Set Validation

The model developed using all of the data points from Phase 3 was validated on 162 samples from all three reservoirs. The model developed (also see Table 21) was in the form of:

$$PC = -479.078 + 210.089(R_{709} / R_{620}) + 82.532(R_{560} / R_{620}) \qquad \text{Equation 15}$$
$$+ 249.717(R_{480} / R_{520})$$

Applying this model to the aggregated validation set resulted in an r^2 value of 0.80 and a RMSE of 28.35 ppb. This was the highest r^2 value and lowest RMSE in the validations.
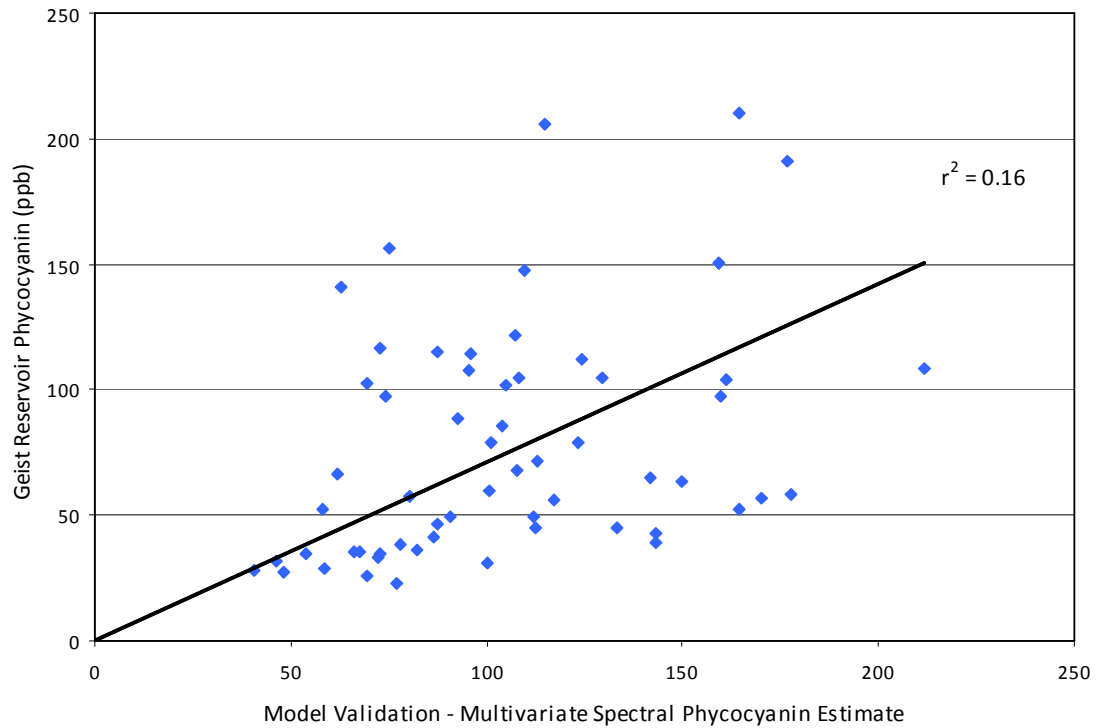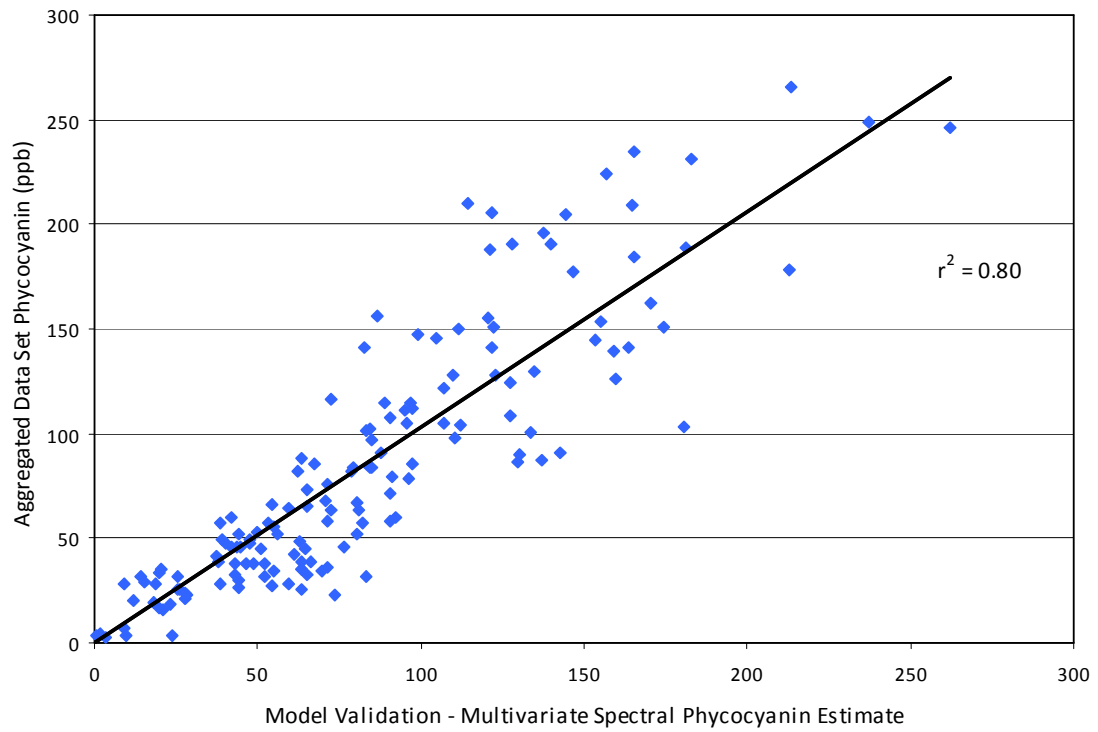
Figure 15. Multivariate phycocyanin spectral estimate versus lab measured phycocyanin concentration for an aggregated data set.

Application of this model, developed using data points from all three reservoirs, performed better on each individual reservoir validation data set than the models developed using individual reservoir data points (Figure 16a-c). A summary of the validation for the aggregated model and individually developed models follows the figures (Table 23).

A - Eagle Creek Reservoir

$r^2 = 0.93$

Phyocyanin (ppb) *(y-axis)*

Multivariate Spectral Phycocyanin Estimate from Aggregated Training Model *(x-axis)*

B - Morse Reservoir

$r^2 = 0.89$

Phycocyanin (ppb) *(y-axis)*

Multivariate Spectral Phycocyanin Estimate from Aggregated Training Model *(x-axis)*
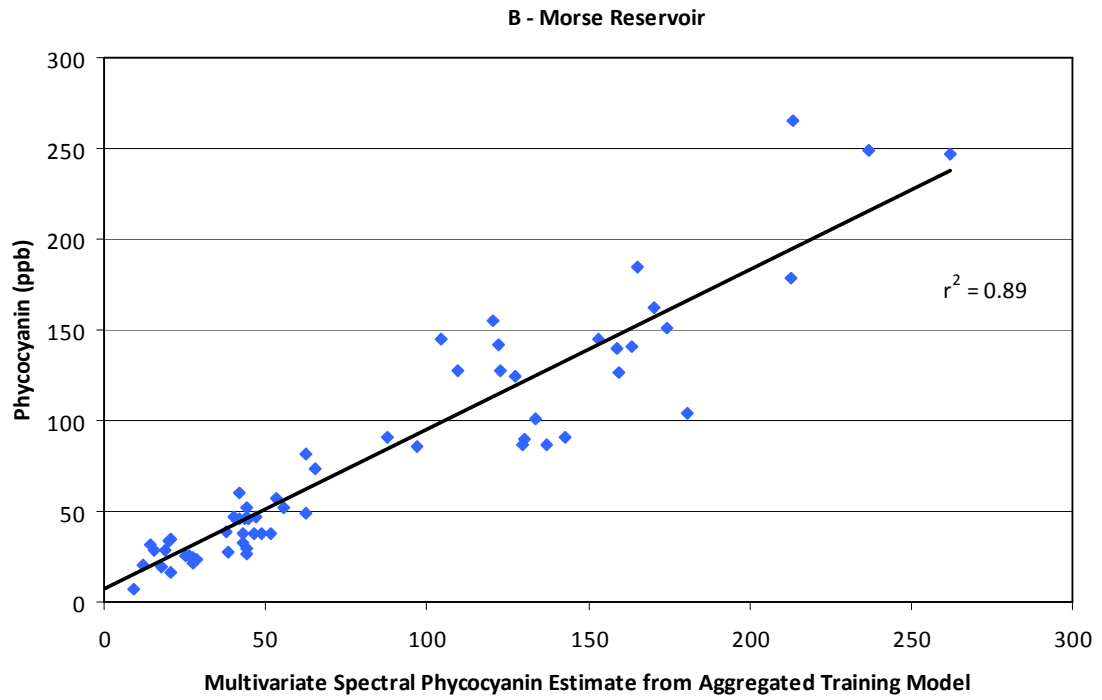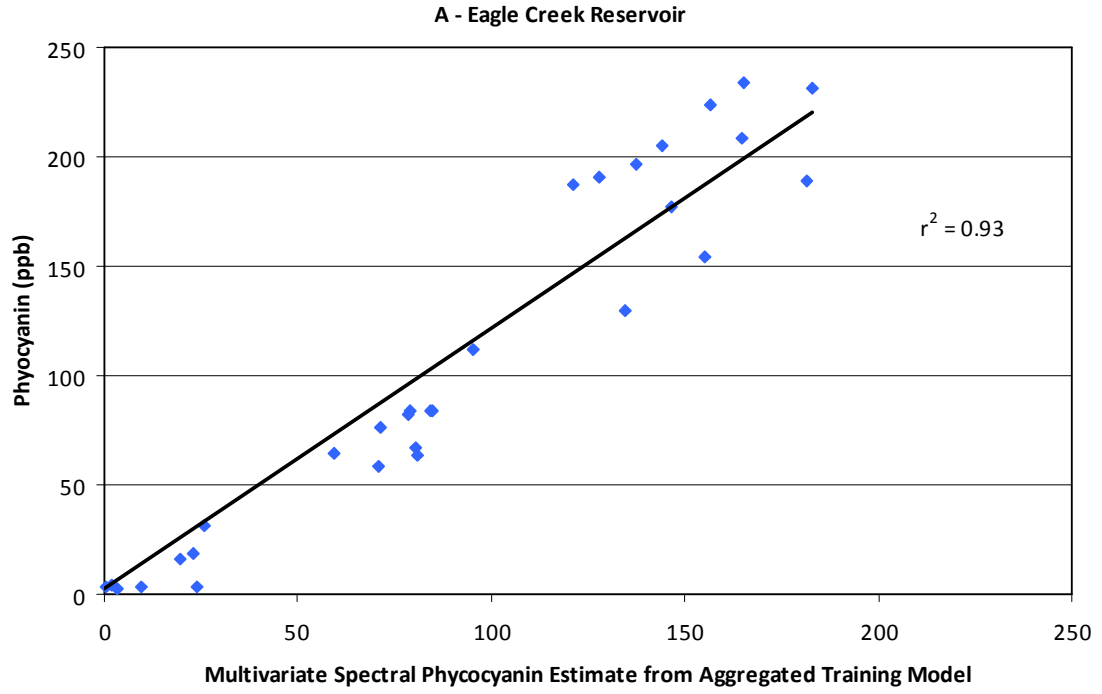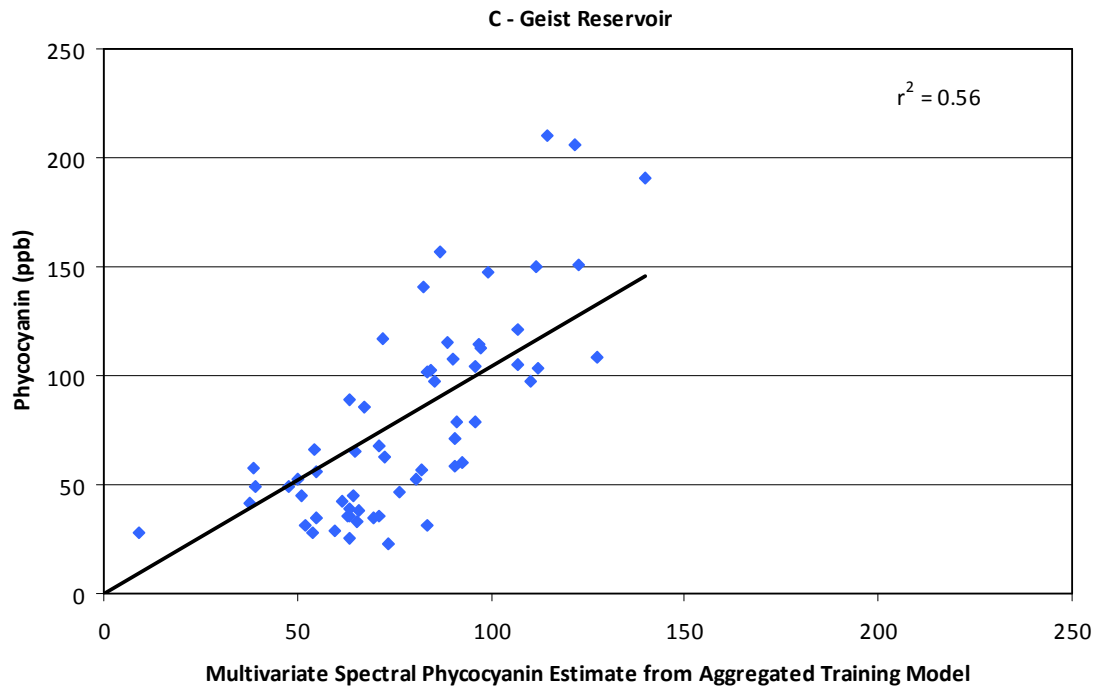
Figure 16a-c. Multivariate phycocyanin spectral model developed on aggregated data set applied to Eagle Creek (a), Morse (b), and Geist (c) validation data sets.

Table 23. Phase 4 results summary.

Reservoir	Model developed on aggregated data set		Model developed on individual reservoir data set	
	r^2	RMSE	r^2	RMSE
Eagle Creek	0.93	31.12	0.78	39.95
Morse	0.89	23.15	0.75	41.31
Geist	0.56	32.15	0.16	54.54
Aggregated	0.80	28.35	-	-

The results suggest using a comprehensive training set created under varying conditions, even across different reservoirs, results in more accurately predictive models for all reservoirs. The improvement was most noticeable for Geist Reservoir. The model developed for Geist Reservoir in Phase 3, using only Geist reservoir data points, had a very poor performance in its validation, despite a strong r^2 value in its development (0.16 in the validation compared to 0.79 when applied to the training set). Applying the model

60

developed in Phase 3 on the aggregated data set resulted in an r^2 value of 0.56 for the Geist Reservoir validation set.

The improvement in the r^2 value is noteworthy. It suggests that the samples used in the Geist Reservoir training are not representative of the samples used in the Geist validation. It is possible samples used in the aggregated data set training model (those from Morse and Eagle Creek) better represent the Geist validation sample set. The samples constituting the Geist training set were samples used in Phase 2 (those samples that had measured values for all of the OACs). In the 2006 data set those were samples that were collected over two days, validated on samples collected on four additional days.

The model developed in Phase 3 on the aggregated data set used samples from three reservoirs collected over a total of 10 days. The variation of water quality conditions captured in the 10 days on the aggregated data set and incorporated in the aggregated training model could explain the improved performance on all three individual reservoir validation sets, particularly for Geist Reservoir. It suggests that the confounding OACs impairing phycocyanin model predictions on Geist Reservoir revealed in the residual analysis are temporally heterogeneous.

V. CONCLUSION

Results of this work validate the use of hyperspectral remote sensing as a tool to estimate phycocyanin concentration in three central Indiana reservoirs.

Correlation of the OACs by reservoir suggests remote sensing models to predict phycocyanin concentration perform best when OACs co-vary. In Eagle Creek Reservoir, phycocyanin was highly correlated to multiple OACs (Table 6). In contrast, phycocyanin was poorly correlated to other OACs in Geist Reservoir, and in the case of total suspended matter and inorganic suspended matter, phycocyanin was negatively correlated. Correlation between phycocyanin and all of the other OACs for Morse Reservoir was positive, though correlation coefficients were not as strong as those measured on Eagle Creek Reservoir.

Regression residual analysis revealed which relationships between OACs and phycocyanin prediction error were statistically significant and the direction of these relationships while holding the effect of the other OACs constant. Its strength was the ability to measure the amount of variation in phycocyanin prediction errors that can be explained by the OACs, and how chlorophyll *a*, ISM, and DOC impact phycocyanin prediction error in water conditions with both high and low phycocyanin concentration.

Analysis of phycocyanin prediction errors revealed strong relationships to sampled optically active constituents, particularly for Geist Reservoir. Regression residual analysis suggested the measured OACs explained 80 to 95% of the phycocyanin prediction error in the tested models for Geist Reservoir. The measured OACs explained less variation in the phycocyanin prediction error for Eagle Creek and Morse Reservoirs. Models assessing phycocyanin prediction error were statistically significant as a whole though, and several OACs were found to be significant confounders for these reservoirs.

Residual analysis informed how OACs impacted error in the phycocyanin spectral estimates, though error could also be introduced through data collection and lab analysis.

Errors in data collection exist if there are changing light conditions during spectra collection. Variation in solar irradiance between on-site calibration and reflectance measurements is possible. Additionally, changes in reflection due to refraction off of the water surface would also introduce error in spectral estimates. Error may also be introduced in analytical analysis. Though several methods for phycocyanin extraction exist, few methods have been validated and no method is widely accepted.

The creation of new multivariate spectral algorithms (Phase 3) to account for confounding constituents had varying success. Though phycocyanin prediction improved, the statistical insignificance of new spectral variables that were statistical confounders demonstrates it is difficult to account for confounding water quality parameters using the algorithms selected for this technique.

The validation of the models on samples not included in model development (Phase 4) revealed the importance of training models on data representing a wide range of water quality conditions. The higher r^2 values and lower RMSE obtained with the model trained on an aggregated dataset for each reservoir reveals the necessity of large training data sets that capture the variation in optically active water parameters a given reservoir exhibits.

Though there is a need for comprehensive ground-truth data, the use of remote sensing to monitor algal blooms is beneficial to water managers. Once a comprehensive spectral library is established and validated, models are easily applicable and can rapidly assess pigment concentration. It is in this way that this application can aid water management in the effective understanding, monitoring, and treatment of degrading blue-green algal blooms.

Works Cited

Astoreca, R., Ruddick, K., Rousseau, V., Van Mol, B., Parent, J., & Lancelot, C. (2006). Variability of the inherent and apparent optical properties in a highly turbid coastal area: impact on the calibration of remote sensing algorithms. EARSel eProceedings.

Bricaud, A., Morel A., & Prieur, L. (1983). Optical efficiency factors of some phytoplankters. *Limnology and Oceanography*, 28 (5), 816-832.

Bricaud, A., Babin, M., Morel, A., & Claustre, H. (1995). Variability in the chlorophyll-specific absorption coefficients of natural phytoplankton: analysis and parameterization. *Journal of Geophysical Research*, 100 (C7), 13321-13332.

Bukata, R.P., Jerome, H.H., Kondatyev, K.Y., & Pozdnyakov, D.V. (1995). *Optical Properties and Remote Sensing of Inland and Coastal Waters*. Boca Raton: CRC Press.

Chorus I. & Bartram, J. (Eds.). (1999). *Toxic cyanobacteria in water: A guide to their public health consequences, monitoring and management*. London: E & FN Spoon.

Dekker, A.G., Malthus, T.J., & Seyhan, E. (1991). Quantitative modeling of inland water-quality for high-resolution MSS systems. *IEEE Transactions on Geoscience and Remote Sensing*, 21 (1), 85-91.

Dekker, A.G. (1993). *Detection of Optical Water Quality Parameters for Eutrophic Waters by High Resolution Remote Sensing*. Ph.D. Thesis. Vrije University Amsterdam.

EPA. (1997). In vitro determination of chlorophyll *a* and pheophytin *a* in marine and freshwater algae by fluorescence. *Method 445.0, Revision 1.2*. Cincinnati, Ohio: U. S. Environmental Protection Agency.

Ferrari, G.M. & Tassan, S. (1992). Evaluation of the influence of yellow substance absorption on the remote sensing of water quality in the Gulf of Naples: a case study. *International Journal of Remote Sensing*, 13, 2177-2189.

Fuli, Y., Shixin, W., Yi, Z., Qing, Z., Weiqi, Z., Lingqa, Z., Xiao, D., Shirong, C., Litao, W., & Pei, Z. (2004). Correlation Analysis of Spectral Reflectance in Determining Preliminary Algorithms for Water Quality Monitoring in Taihu Lake, China. Institute of Remote Sensing Applications, Chinese Academy of Sciences.

Gin, K.Y.-H., Koh, S.T., & Lin, I.I. (2003). Spectral irradiance profiles of suspended marine clay for the estimation of suspended sediment concentration in tropical waters. *International Journal of Remote Sensing*, 24, 3235-3245.

Gitelson, A. (1992). The peak near 700 nm on radiance spectra of algae and water: relationships of its magnitude and position with chlorophyll concentration. *International Journal of Remote Sensing*, 13, 3367-3373.

Gitelson, A., Garbuzov, G., Szilagyi, F., Mittenzwey, K.H., Karnieli, A., & Kaiser, A. (1993). Quantitative remote sensing methods for real-time monitoring of inland waters quality. *International Journal of Remote Sensing*, 14, 1269-1295.

Gitelson, A.A., Laorawat, S., Keydan, G.P., & Vonshank, A. (1995). Optical properties of dense algal culture outdoors and their application to remote estimation of biomass and pigment concentration in Spirulina Platensis (Cyanobacteria). *Journal of Phycology*, 31, 828-834.

Gitelson, A.A., Yacobi, Y.Z., Schalles, J.F., Rundquist, D.C., Han, L., Stark, R., & Etzion, D. (2000). Remote estimation of phytoplankton density in productive waters. *Archiv fuer Hydrobiologie- Special Issues Advancements in Limnology*, 55, 121-136.

Gitelson A., Schalles, J.F., & Hladik, C.M. (2007). Remote chlorophyll-a retrieval in turbid, productive estuaries: Chesapeake Bay case study. *Remote Sensing of Environment*, 109, 464-472.

Gons, H. (1999). Optical teledetection of chlorophyll *a* in turbid inland waters. *Environmental Science Technology*, 33, 1127-1132.

Gordon, H., Brown, O., & Jacobs, M. (1975). Computed relationships between the inherent and apparent optical properties of a flat homogeneous ocean. *Journal of Applied Optics*, 14, 417-427.

Hamill, K.D. (2001). Toxicity in benthic freshwater cyanobacteria (blue-green algae): first observations in New Zealand. *New Zealand Journal of Marine and Freshwater Research*, 35, 1057-1059.

Han, L., Rundquist, D.C., Liu, L.L., Fraser, R.N., & Schalles, J.F. (1994). The spectral response of algal chlorophyll in water with varying levels of suspended sediments. *International Journal of Remote Sensing*, 15, 3707-3718.

Han, L. & Rundquist D.C. (1996). Spectral characterization of suspended sediments generated from two texture classes of clay soil. *International Journal of Remote Sensing*, 17, 643-649.

Horne, A.J. & Goldman, C.R. (1994). *Limnology* (2nd ed.). New York: McGraw Hill, Inc.

Kirk, J.T.O. (1994). *Light and photosynthesis in aquatic ecosystems*. Cambridge: Cambridge University Press.

Kutser, T., Pierson, D.C., Kallio, K.Y., Reinart, A., & Sobek, S. (2005). Mapping lake CDOM by satellite remote sensing. *Remote Sensing of the Environment*, 94, 535-540.

Li, L., Pascual, D.L., Tedesco, L.P., Randolph, K.L., Sengpiel, R.E., Hall, B.E., Wilson, J.S. (2006). *Developing a survey tool for the rapid assessment of blue-green algae in central Indiana's reservoirs.* IUPUI. Indianapolis: Central Indiana Resources Partnership / CEES.

Liu, Y., Islam Md.A., & Gao, J. (2003). Quantification of shallow water quality parameters by means of remote sensing. *Progress in Physical Geography*, 27, 1, 24-43.

Millie, D.F., Baker, M.C., Tucker, C.S., Vinyard, B.T., & Dionigi, C.P. (1992). High-resolution airborne remote sensing of bloom-forming phytoplankton. *Journal of Phycology*, 28, 281-290.

Morel, A. & Prieur, L. (1977). Analysis of variations in ocean color. *Limnology and Oceanography*, 22, 709-722.

Morel, A. & Gordon, H. R. (1980). Report of the Working Group on Water Color. *Boundary-Layer Meteorology*, 18, 343-355.

Morel, A. (2001). Bio-optical Models. In J.H. Steele, K.K. Turekian & S.A. Thorpe (Eds.), *Encyclopedia of Ocean Sciences*. (pp. 317-326). New York: Academic Press.

Novo, E.M.L.M., Hansom, J.D., & Curran, P.J. (1989). The effect of sediment type on the relationship between reflectance and suspended sediment concentration. *International Journal of Remote Sensing*, 10, 1283-1289.

Pitois, S., Jackson, M., & Wood, B. (2000). Problems Associated with the presence of cyanobacteria in recreational and drinking waters. *International Journal of Environmental Health Research*, 10, 203-218.

Randolph, K.L. (2007). Remote Sensing of Cyanobacteria in Case II Waters using Optically Active Pigments, Chlorophyll *a* and Phycocyanin. Master's Thesis. Indiana University-Purdue University Indianapolis.

Rowan, K.S. (1989). *Photosynthetic Pigments of Algae.* Cambridge: Cambridge University Press.

Sarada, R., Pillai, M.G., & Ravishankar, G.A. (1999). Phycocyanin from *Spirulina* sp: influence of processing of biomass on phycocyanin yield, analysis of efficacy of extraction methods and stability studies on phycocyanin. *Process Biochemistry*, 34, 795-801.

Schalles, J.F., Schiebe, F.R., Starks, P.J., & Troeger, W.W. (1997). Estimation of algal and suspended sediment loads (singly and combined) using hyperspectral sensors and experiments. *Proceedings of the Fourth International Conf. on Remote Sensing of Marine and Coastal Environments*, 1, 247-258.

Schalles, J.F. & Yacobi, Y.Z. (2000). Remote detection and seasonal patterns of phycocyanin, carotenoid and chlorophyll pigments in eutrophic waters. *Archiv fuer Hydrobiologie-Special Issues Advancements in Limnology*, 55, 153-168.

Schalles, J. (2006). Optical Remote Sensing Techniques to Estimate Phytoplankton Chlorophyll *a* Concentrations in Coastal Waters with Varying Suspended Matter and CDOM Concentrations. In L.L. Richardson & E.F. LeDrew (Eds.), *Remote Sensing of Aquatic Coastal Ecosystem Processes: Science and Management Applications* (pp. 27-79). Netherlands: Springer.

Sengpiel, R.E. (2007). Using Airborne Hyperspectral Imagery to Estimate Chlorophyll *a* and Phycocyanin in three Central Indiana Mesotrophic to Eutrophic Reservoirs. Master's Thesis. Indiana University-Purdue University Indianapolis.

Simis, S.G., Peters, S.W., & Gons, H. (2005). Remote Sensing of the cyanobacterial pigment phycocyanin in turbid inland water. *Limnology and Oceanography*, 50, 237-245.

Strombeck, N. (2001). Water Quality and Optical Properties of Swedish Lakes and Coastal Waters in Relation to Remote Sensing. Master's Thesis. Uppsala University Uppsala.

Tedesco, L.P., Atekwana, E.A, Filippelli, G., Licht, K., Shrake, L.K., Hall, B.E., Pascual, D.L., Latimer, Raftis, R., Sapp, D., Lindsey, G., Maness, R., Pershing, D., Peterson, D., Ozekin, K., Mysore, C., & Prevost, M. (2003). *Water Quality and Nutrient Cycling in Three Indiana Watersheds and Their Reservoirs: Eagle Creek/Eagle Creek Reservoir, Fall Creek/Geist Reservoir and Cicero Creek/Morse Reservoir*. IUPUI. Indianapolis: Central Indiana Water Resources Partnership / CEES Publication 2003-01.

Vertucci, F.A., & Likens, G.E. (1989). Spectral Reflectance and water quality of Adirondack mountain region lakes. *Limnology and Oceanography*, 34, 1656-1672.

Vodacek, A., Blough, N.V., DeGrandpre, M.D., Peltzer, E.T., & Nelson, R.K. (1997). Seasonal variation of CDOM and DOC in the Middle Atlantic Bight: Terrestrial inputs and photooxidation. *Limnology and Oceanography*, 42 (4), 674-686.

Warrick, J.A., Mertes, L.A., Siegel, D.A, & Mackenzie, C. (2004). Estimating Suspended Sediment Concentrations in Turbid Coastal Waters of the Santa Barbara Channel with SeaWiFS. *International Journal of Remote Sensing*, 25, 1995-2002.

Yacobi, Y.Z. (2006). Temporal and vertical variation of chlorophyll a concentration, phytoplankton photosynthetic activity and light attenuation in Lake Kinneret: possibilities and limitations for simulation by remote sensing. *Journal of Plankton Research*, 28 (8), 725-736.

Zimba, P.V. & Gitelson A. (2006). Remote estimation of chlorophyll concentration in hyper-eutrophic aquatic systems: Model tuning and accuracy optimization. *Aquaculture*, 256, 272-286.

APPENDIX A

Summary of Analytical Methods

Sample	Analytical Method	Detection Limit	Method Description	Description
Alkalinity (mg/L as CaCO3)	EPA (310.1)	2.0	Titrametric	Alkalinity by titration to pH 4.5. Acid neutralizing capacity (sum of all titratable bases). Primarily a function of carbonate, bicarbonate, and hydroxide content (usually an indicator of the concentration of these consituents)
DOC (mgC/L)	SM (5310C)	0.5	Persulfate	Oxidation-Amount of TOC that passes through a 0.45µm-pore-diam filter
TOC (mgC/L)	SM (5310C)	0.5	Persulfate	Oxidation-Persulfate and Ultraviolet Oxidation with IR detection. Carbon atoms covalently bonded in organic molecules are broken down to be measured quantitatively. Organic Carbon is oxidized into CO_2 by persulfate using UV light. CO_2 is removed from the sample, dried, and transferred with a carrier gas to an IR analyzer.
Chloride (mg/L)	EPA (300.0)	8.0	Ion	Method 300.0 is an ion chromatograph method using a Dionex DX-600 system with a conductivity detector. Sample is added to an ion chromatograph. Anions are separated and measured using a gaurd column, analytical column, supressor device, and conductivity detector.
Sulfate (mg/L)	EPA (300.0)	8.0	Ion	Method 300.0 is an ion chromatograph method using a Dionex DX-600 system with a conductivity detector. Sample is added to an ion chromatograph. Anions are separated and measured using a gaurd column, analytical column, supressor device, and conductivity detector.
O-Phos (mg/L)	EPA (300.0)	0.05	Ion	Method 300.0 is an ion chromatograph method using a Dionex DX-600 system with a conductivity detector. Sample is added to an ion chromatograph. Anions are separated and measured using a gaurd column, analytical column, supressor device, and conductivity detector.
Total P (mg/L)	SM (4500-P E.)	0.010	Colorimetric	Ascorbic Acid Colorimetric method-Ammonium molybdate and potassium antimonyl tartrate react in acid with orthophosphate to form phosphomolybdic acid that is reduced to colored moltybdenum blue by ascorbic acid.
Nitrite (mg/L)	EPA (300.0)	0.0	IC	Method 300.0 is an ion chromatograph method using a Dionex DX-600 system with a conductivity detector. Sample is added to an ion chromatograph. Anions are separated and measured using a gaurd column, analytical column, supressor device, and conductivity detector.
Nitrate (mg/L)	EPA (300.0)	0.10	IC	Method 300.0 is an ion chromatograph method using a Dionex DX-600 system with a conductivity detector. Sample is added to an ion chromatograph. Anions are separated and measured using a gaurd column, analytical column, supressor device, and conductivity detector.
NH4-N (mg/L)	SM (4110)	0.02	IC	Sample injected into carbonate-bicarbonate and passed through series of ion exchangers. Anions are separated by their relative affinities for for a strongly basic anion exchanger. Anions passed through s fiber supressor coated with a strong acid solution to conv ert anions to highly conductive acid form, conductivity is measured. Concentration is determined from measurement of peak height or area.
TKN (mg/L)	EPA (351.4)	0.30	Contracted Out	Determined by digestion, followed by ammonia determination by ion selective Electrode by a contract lab

Sample	Analytical Method	Detection Limit	Method Description	Description
Silica (mg/L) unfiltered	EPA (370.1)	0.10	Colorimetric	Heteropoly acids are produced by the addition of Ammonium molybdate (at pH 1.3) to sample containing silica and phosphates. Molybdosilicic acid is preserved and molybdphosphoric destroyed with the addtion of oxalic acid. Intensity of yellow color is indicative of concentration of molybdate-reactive silica.
Ca (mg/L)	EPA (300.7)	3.0	IC	Method 300.0 is an ion chromatograph method using a Dionex DX-600 system with a conductivity detector. Sample is added to an ion chromatograph. Anions are separated and measured using a gaurd column, analytical column, supressor device, and conductivity detector.
Mg (mg/L)	EPA (300.7)	1.0	IC	Method 300.0 is an ion chromatograph method using a Dionex DX-600 system with a conductivity detector. Sample is added to an ion chromatograph. Anions are separated and measured using a gaurd column, analytical column, supressor device, and conductivity detector.
K (mg/L)	EPA (300.7)	0.05	IC	Method 300.0 is an ion chromatograph method using a Dionex DX-600 system with a conductivity detector. Sample is added to an ion chromatograph. Anions are separated and measured using a gaurd column, analytical column, supressor device, and conductivity detector.
Na (mg/L)	EPA (300.7)	1.0	C	Method 300.0 is an ion chromatograph method using a Dionex DX-600 system with a conductivity detector. Sample is added to an ion chromatograph. Anions are separated and measured using a gaurd column, analytical column, supressor device, and conductivity detector.
Total Hardness (mg)	SM (2340 B)	12.0	Calculation	Total hardness is calculated from the sum of Calcium and Magnesium Concentrations (mg CaCO3/L)
MIB (ng/L)	SM (6040)	3.0	Mass Spectrometric	Organics are extracted from water by closed-loop stripping. Extracted organics are injected into a gas chromatograph/mass spectrometer for identification based on retention time and spectrum comparison. Single-ion current integration is used to quantify MIB.
Geosmin (ng/L)	SM (6040)	3.0	Mass Spectrometric	Organics are extracted from water by closed-loop stripping. Extracted organics are injected into a gas chromatograph/mass spectrometer for identification based on retention time and spectrum comparison. Single-ion current integration is used to quantify Geosmin.

Curriculum Vitae

Lara Anne Vallely

Education
Geographic Information Science, M.S.
Indiana University, Indianapolis, IN, July 2008

Agriculture and Natural Resources, B.S., *Summa cum laude*
Berea College, Berea, KY, December 2003
Minors: Sustainability and Environmental Studies, Women's Studies

Funding
University Fellowship, Indiana University, 2006 – 2007
Research Assistantship, Center for Earth and Environmental Science, IUPUI, 2007 – 2008

Professional Experience
Research Assistant, IUPUI
      Center for Earth and Environmental Science,   June 2007 – May 2008
      Remote sensing of water quality

      Deparment of Geography,   January 2006 – July 2007
      Remote sensing based atlas of the Caribbean

      School of Public and Environmental Affairs,   January 2007 – May 2007
      Data compilation of Indianapolis Heritage Trail

Conference and Meeting Presentations
Vallely, L.A., Wilson, J.S., Lin, L., and Tedesco, L.P. Assessing Empirical and Semi-Empirical Algorithms to Estimate Phycocyanin in Three Central Indiana Reservoirs. Central Indiana Water Resources Partnership, April 2008 Meeting, Indianapolis, IN.

Tedesco, L.P., Lin, L., Wilson, J.S., Vallely, L.A., Robertson, A.L., Pascual, D.L., Randolph, K.L., and Sengpiel, R.E. Remote Sensing of Cyanobacteria in Central Indiana Reservoirs: A Diagnostic and Management Tool. Central Indiana Water Resources Partnership, January 2008 Meeting, Indianapolis, IN.

Vallely, L.A., Wilson J.S., Tedesco, L.P., Pascual, D.L., Randolph K.L., Li L., and Cigana J. Remote Sensing of Blue-Green Algae for Water Quality Management. Poster presented at the Great Midwestern Regional Space Grant Consortia Conference, September 2007, West Lafayette, IN.

Vallely, L.A. Exploring the Utility of the Remote Sensing Archive for an Indiana Wetland Restoration Site. Poster presented at the American Association of Geographers Annual Conference, April 2007, San Francisco, CA.